SURFACE FUNCTIONALIZATION OF NANODIAMONDS USING THE BIOMACROMOLECULE CHITOSAN (CS)

by

LEWIS Q. LOTT

A THESIS

Submitted in partial fulfillment of the requirements
for the degree of Master of Science in the
Applied Chemistry Graduate Program
of Delaware State University

DOVER, DELAWARE
May 2017

The following members of the Final Oral Review Committee approve this thesis:

Dr. Cherese Winstead, Committee Chairperson, Department of Chemistry, Delaware State University
Dr. Daniela Radu, Committee Member, Department of Chemistry, Delaware State University
Dr. Andrew Goudy, Committee Member, Department of Chemistry, Delaware State University
Dr. Hacene Boukari, External Committee Member, Department of Chemistry, Delaware State University

DEDICATION

I would like to dedicate this thesis to my fiancé, Bithiah Sam, my parents, both of my grandmothers, my siblings, and my friends, who were all there showing support for me throughout the duration of achieving my goals.

ACKNOWLEDGEMENT

My deepest gratitude goes out to my advisor Dr. Cherese Winstead for helping me develop into the scientist that I am today. She has spent the time that she has had, offering her patience, guidance, encouragement, making suggestions, and giving positive criticisms in preparation for my future endeavors. Without her support, her expertise, research insights and diligence, there would not have been a way for me to accomplish my goal of completing this research successfully. I can truly say that I am humbled to have had worked with a great advisor, such as her.

I am thankful for my committee members, Dr. Andrew Goudy, Dr. Hacene Boukhari, and Dr. Daniela Radu for offering their support in my endeavors towards completing this research.

I want to give a special thanks to my mentor, Dr. Kimberly Milligan, for believing in me and offering encouragement in times when it seemed I needed it most. Sincerely, my appreciation goes out to the faculty members, from the custodians, to all the professors for helping me to become the greatest researcher/professional that I could possibly be in the mere future.

I would like to express my deepest appreciations to Dr. Yury Gogotsi of Drexel University, Mr. Gerald Poirier of the University of Delaware, and Mrs. Deborah Powell of the Delaware Biotechnological Institution for their willingness to open their labs and help support my endeavors as a student scholar.

I am in debt to the Louis Stokes Alliance for Minority Programs Bridge to the Doctorate Fellowship, and the NSF Grant (#1458980) for funding and supporting me throughout the duration of completing the Applied Chemistry Master's Degree here at DSU.

"Now unto Him whom is able to do exceedingly, and abundantly above all that we ask or think, according to the power that worketh in us" [Ephesians 3:20]; my biggest and humblest gratitude goes to my Lord and savior, Jesus the Christ.

SURFACE FUNCTIONALIZATION OF NANODIAMONDS USING THE BIOMACROMOLECULE CHITOSAN (CS)

Lewis Q. Lott

Faculty Advisor: Dr. Cherese Winstead

ABSTRACT

NDs are highly promising drug delivery vehicles (DDVs) due to the materials low cytotoxicity and biocompatibility. The advantage of these materials lies within their tunable surface chemistry and inherent optical properties. Despite the numerous benefits, the use of NDs in biological systems is impeded by their high aggregation propensity in polar liquid medium, a caveat from its rich chemistry. ND particles typically aggregate into much larger groups >200 nm, which are too large for drug delivery applications. In this work, salt assisted attrition milling was utilized to decrease ND aggregates. After 5 hours of milling, dynamic light scattering (DLS) measurements revealed a maximum particle distribution at 127 nm, with significant reduction in the mass fraction of larger particle size distribution from 300-1000nm. The average size of the nanodiamond particles was also shown to increase with an increasing concentration of chitosan (0.25 w/v%; 142nm and 1 w/v%; 825nm). In the modification of nanodiamonds, FTIR was used to examine the chemical composition of the nanodiamonds, both before and after functionalization. FTIR results of the pristine nanodiamonds showed characteristic bands at 3400cm^{-1} (-OH) 1630 cm-1 (C=O) and 1080 (-C-O). Chitosan exhibited spectral regions of interest at 3350 cm^{-1} (-OH), 1665 cm^{-1} (NH_2) and 1030 cm^{-1} (C-O). Successful functionalization

of the nanodiamaond surface was confirmed by the appearance of the amide band I at 1664 cm^{-1} and presence of strong C-O stretching at 1197cm^{-1} from the chitosan backbone. This is indicative of the covalent binding of NH_2 on chitosan with COOH on the ND surface. X-ray diffraction was performed to observe the structure and crystallinity of the NDs and showed crystalline characteristic peaks at 2Θ 44º (111), 75º (220), and 91º (113) for the pristine ND. The appearance of an amorphous band at 2Θ 22º in the analysis of ND-COOH-CS is indicative of the surface modification of the nanodiamond with the biopolymer, CS. Zeta potential analysis show an increase in the zeta potential with an increase in concentration of CS (pristine ND, -40mV; 0.25 w/v%, -26.7mV; and 1 w/v%; 12.9mV). This increase in zeta potential is indicative that a more stable dispersion of nanodiamonds was created upon functionalization with the biopolymer, CS. TGA was also used to confirm the composition of the pristine and modified NDs. Loss of water was observed initially for all samples at 100C followed by onsets of degradation for CS and ND-COOH-CS occurred at 212°C and 232.16 °C for CS and ND-COOH-CS, respectively. The presence of weight loss profiles characteristic of CS in the ND-COOH-CS thermogram confirmed modification of the ND surface when compared to the pristine ND. Morphological investigations of the nanodiamonds using TEM showed a particle size of ~150-300nm supporting PSA results. TEM images also showed characteristic aggregation of the NDs due to the presence of attractive surface functional groups. This work confirms the capability of surface functionalization of nanodiamonds using biomacromolecules and reveals the potential application regarding the use of these materials as DDVs with enhanced permeability and compatibility properties.

TABLE OF CONTENTS

Page

LIST OF TABLES

Page

LIST OF FIGURES

Page

LIST OF ABREVIATIONS

NDs	**Nanodiamonds**
DNDs	**Detonated Nanodiamonds**
DDVs	**Drug Delivery Vehicles**
DDS	**Drug Delivery System**
DLS	**Dynamic Light Scattering**
FTIR	**Fourier Transform Infrared Spectroscopy**
XRD	**X-Ray Diffraction**
TGA	**Thermogravimetric Analysis**
TEM	**Transmission Electron Microscopy**
ZPA	**Zeta Potential Analysis**
ATR	**Attenuated total reflection Infrared Spectroscopy**
TFA	**Trifluoroacetic Acid**
CCS	**Cross Correlation Spectrophotometry**
CS	**Chitosan (β-1,4-linked N-acetyl-D-glucosamine (GlcNAc))**
pNDs	**Pristine Nanodiamonds**
ND-COOH	**Carboxylated Nanodiamonds**
ND-COOH-CS	**Carboxylated Nanodiamond-Chitosan Composite**
(NV)	**Nitrogen Vacancy Center**
(NV^0)	**Neutrally Charged Nitrogen Vacancy Center**
(NV^-)	**Negatively Charged Nitrogen Vacancy Center**

NVN **Nitrogen Vacancy Nitrogen (H3) center**

CHAPTER 1
INTRODUCTION

1.1 OVERVIEW OF NANOTECHNOLOGY

Nanotechnology is a rapidly expanding field, dealing with the development of nano-sized materials, along with the techniques and equipment functioning at the nano-scale. These materials and devices can be designed to interact with cells and tissues at a molecular (i.e. subcellular) level with high degree of functional specificity, thus allowing integration between the device and biological system, not previously attainable.[1] The field of nanotechnology bridges the discipline of physics, chemistry, and biology and manipulates the chemical physical properties of a substance on a molecular level.

Requirements of a nanomaterial are that at least one dimension of the nanomaterial should be from 1 through 100 nm, or the nanomaterial should show novel nano-scale characteristic(s) of the bulk material.[1] Since aggregation and functionalization can have a substantial effect on the size of some of the particles to exclude them from the nano category, the dimensions of the internal structure of particle have been included in the definition. [1] For biological applications, the size of nanomaterials usually ranges from 5 to 250 nm.[1-3] Some researchers and organizations such as FDA classify nanomaterials as those under the size of 1000 nm.[1-5]

Today, nanotechnology is gaining importance in biomedical field due to its small size and targeted effects. Due to their larger surface area relative to their volume, leading to an increase in their reactivity compared to micro and macro particles. The field of technology encompasses a

vast range of materials, such as metals (gold, silver), metal oxides, [e.g. titanium dioxide (TiO2), Silicon dioxide (SiO2)], inorganic materials (carbon nanotubes, quantum dots), polymeric materials and lipids.[5-7] Nanomaterials take the forms of nanoparticles, nanofibers, nanocrystals, cantilevers, dendrimers, nanoshells and nanowires.[6-9] Products made from each of these nanomaterials can be used for diagnosis (as biomarkers) and therapy. Nanoparticles, for example can have multiple functionalities that can provide detailed information on the progression of disease. There is also a dominance of quantum effects at the nano-size, which affects their optical, electrical, thermal, and magnetic behavior.[3] For example, gold particles differ considerably in their color, melting point and catalytic effects depending upon their size. [5-9]

1.2 CANCER THERAPY

Cancer is a group of diseases characterized by the uncontrolled growth and spread of abnormal cells.[10] Currently detection and diagnosis of cancer usually depends on changes in cells and tissues which occur at the nanoscale level inside the cells and are detected either by physical examination or imaging expertise.[10] It is of upmost importance that cancer is detected when the earliest molecular changes occur. If the spread is not controlled, it can result in death. External factors cause cancer, such as tobacco, infectious organisms, and an unhealthy diet, and internal factors, such as inherited genetic mutations, hormones, and immune conditions.[10-11] These factors may act together or in sequence to cause cancer. Treatments include surgery, radiation, chemotherapy, hormone therapy, immune therapy, and targeted therapy (drugs that specifically interfere with cancer cell growth).[10]

Surgery is the most widely used treatment available for cancer patients and is used when there is a good chance to remove an entire tumor before it spreads.[12] Surgery is rarely used as a

stand-alone treatment but usually combined with radiation therapy and /or chemotherapy. In radiation therapy, the specific part of the body containing a cancerous growth is exposed to radiation energy to attack reproducing cancer cells.[10-12] Radiation therapy is often used to shrink a tumor so that it can be removed through surgery, or to prevent tumor growth following surgery.[10-12] However, the radiation cannot affect the cancer cells without affecting normal cells, which can lead to several unpleasant side effects. Chemotherapy, the treatment of cancer through drugs, is an effective treatment method for fighting cancerous cells that have spread to other parts of the body and that cannot be treated with any other method.[12-14] Like radiation therapy, chemotherapy also can affect normal cells, causing adverse side effects. Hormone therapy involves manipulating the body's hormones to treat the cancer, including administering hormones and drugs.[12-14] Immunotherapy also manipulates the body's normal functions to stimulate the body's immune system to fight cancerous cells.[12-14]

1.3 CHALLENGES IN CANCER THERAPY

Cancer is represented mostly by heterogeneous diseases which cause uncontrolled growth and spreading of irregular cells, that lead ultimately to cell death.[15-20] Side-effects are often caused by the major issues that are a result of anti-cancerous drugs due to a broad uptake by healthy cells.[20-22] Many effective drugs used to treat cancer diseases are not soluble in polar protic solvents, such as water; thus, they pose a challenge in delivery.[14] Other major challenges are the discovery of anticancer drugs concerning tumor heterogeneity, the vital and nonessential target zones, and the focus on selective versus nonselective multi-targeting drugs used on different patients.[22] Additional limitations in the use of therapeutic drugs include multidrug resistance (MDR) which discharges the effectiveness of the drug with chemotherapy.[23] As a

consequence of these difficulties in targeting the appropriate cancer cells, nanomedicine has emerged.

1.4 NANOTECHNOLOGY IN BIOMEDICINE

Studies have shown, that drugs cannot effectively target endocytic surfaces.[24] Thus, there is a need for technologies that can facilitate the transport drugs intracellularly. Currently, the most promising consequence of the application of nanotechnology, with respect to medicine, is of drug delivery. The major problem with most of the new chemical entities is their insolubility.[20] Therefore, the first principal aim of nanotechnology is to improve their solubility and bioavailability. The second is to enhance the release rate of the drug. Due to these reasons nanotechnology has focused on targeted drug delivery and controlled drug release.[11,12] A targeted drug delivery system can convey drugs more effectively, increase patient compliance and extend product life cycle. According to Dubin [12], drugs tend to perform more effectively in nanoparticulate form and with fewer side-effects. Further, specific nanosized receptors present on the surface of a cell can recognize the drug and elicit an appropriate response, by delivering and releasing therapy exactly wherever needed.[12,24]

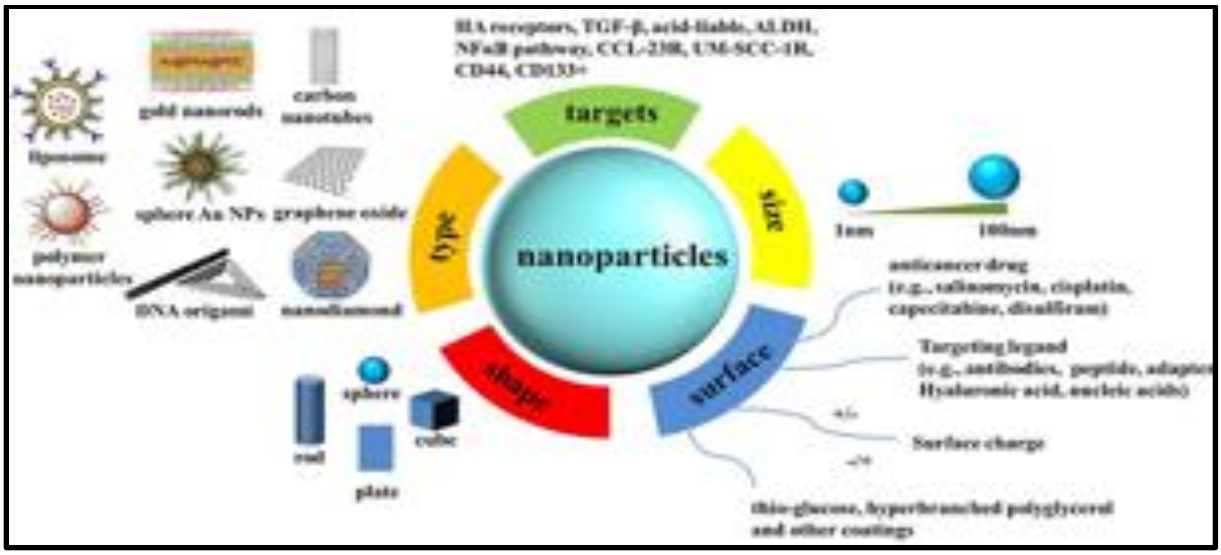

Figure 1.4 Applications of nanotechnology and parameters of drug delivery [15]

1.5 NANOTECHNOLOGY AND CANCER THERAPY

Nanotechnology offers a wealth of tools that provide cancer researchers with new and innovative ways to diagnose and treat cancer.[2-3] For example, nanoscale devices can deliver multiple therapeutic agents to a tumor in order to simultaneously attack multiple points in the pathway involved in cancer.[2] Similarly, nanotechnology generates in vivo biosensors that have the capability of detecting and pointing the location of tumor and metastatic changes that are smaller than those detectable using conventional technologies.[2]

After diagnosis when it is time to treat cancer, nanoscale devices have the potential to improve cancer therapy vs. existing conventional (chemotherapy, radiotherapy) techniques and to discover new therapeutic agents .[3-5] It is useful for developing ways to eradicate cancer cells without harming healthy, neighboring cells. A major focus in the field of nanotechnology is to create therapeutic agents that can target specific cells and deliver toxins in a controlled, time

released manner.[6] The goal of researchers is to find out agents of these nanoparticles which can circulate through the body, detect cancer associated molecular changes, assist in imaging, release a therapeutic agent and then monitor the effectiveness of the intervention.[5-6] It can reduce the unpalatable side-effects that accompany many current cancer therapies.[3-5]

1.6 CURRENT NANOCARRIERS

Nanotechnology incorporation with cancer research has made groundbreaking results in the areas of detectability, biomarkers used to identify diseases, and the innovation in imaging agents.[2,20] Over the past decades, nanoformulation has been the focus of many nanocarrier research to drive drugs into specific locations without causing harm. Nanocarriers are nanomaterials used to successfully facilitate drug delivery. The family of nanocarriers include dendrimers, nanocrystals, nanoshells, carbon nanotubes (C-NT), and nano-liposomes.[26-30] The dendrimer form of nanotechnology is unique due to its branching shape, which provides a vast surface area so that therapeutic agents or other biological molecules may be attached. Nanoshells, another recent invention, are miniscule beads coated with gold. These beads can be designed to absorb specific wavelength of light.[26] The absorption of light by the nanoshells creates an intense heat that is lethal to the cells.[26] Liposomes are small spherical systems that are synthesized from cholesterol and non-toxic phospholipids in the body.[27] Liposomes are natural materials considered as attractive, harmless drug delivery carriers that can circulate in the blood stream for a long time.[27] The form of carbon nanotubes enables easy penetration through cells.[25,26] The special structures on the surface of carbon nanotubes offer opportunities for either non-covalent or covalent bonding to therapeutic agents that have poor membrane penetrability such as: peptides, small molecule drugs, and protein drugs or DNA.[25,26] Common nanocarriers

currently in trial in the field of oncology include: PEGylated colloidal gold nanoparticles, called Aurimune,[25] AP5280, which is composed of a HMPA copolymer with a platinum complex.[28]

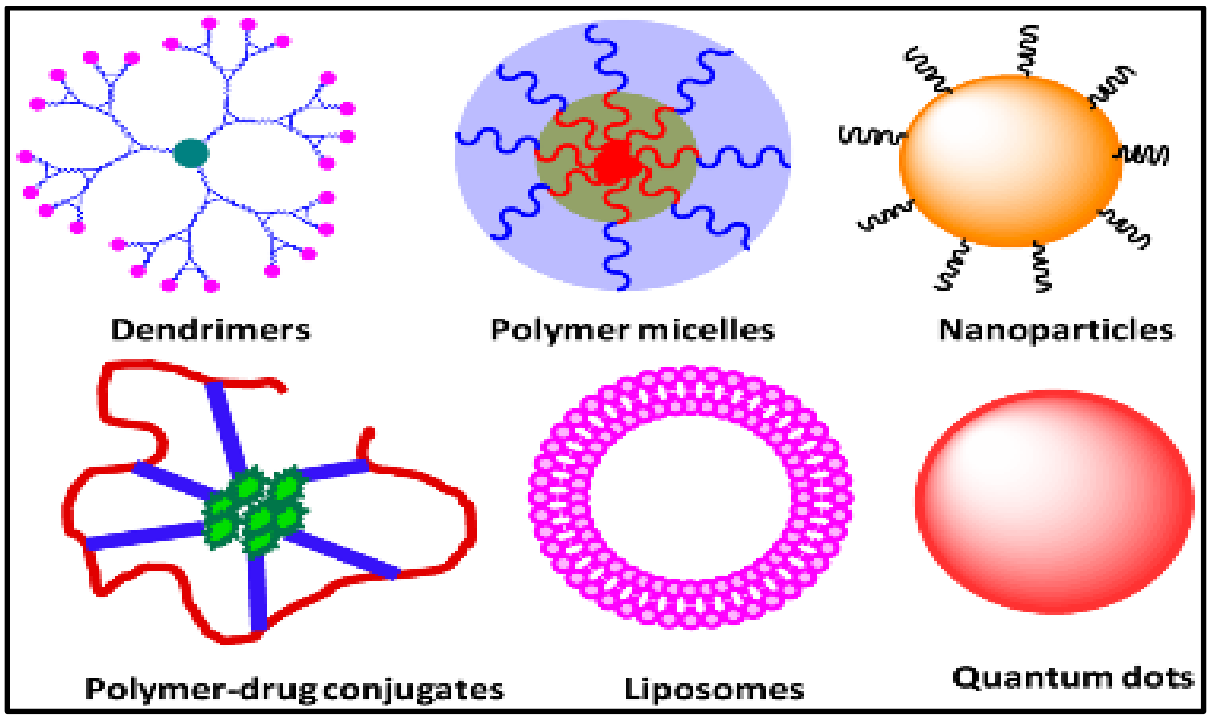

Figure 1.8 Common Nanocarriers used in Biomedicine.[26]

1.7 CRITICAL PARAMETERS IN THE DEVELOPMENT OF DRUG DELIVERY SYSTEMS (DDS)

There is an ever-increasing need for advanced nanotechnology with the enhanced properties of solubility, transport, and stability. The physiochemical properties of various nanomaterials such as size, zeta potential and aggregation have a substantial effect on the behavior of the ideal nano drug delivery system (DDS). Therefore, these parameters should be controlled and characterized critically, and are discussed in this work.

1.7.1 SIZE

One of the strategies for effective drug delivery is size of the carrier. Rapid clearance from the biological system occurs when the nanomaterial is greater than 200 nm.[28-30] Alternatively, if the particles are too small, less than 5 nm, they will be excreted.[28-29] The size range between 100 to 300 nm for the nanocarrier is suggested to have the highest potential for the efficient cellular interaction, uptake, and release.[29-31]

1.7.2 SURFACE CHARGE

Nanocarriers with highly anionic backbones suffer from poor interaction with the negatively charged cell surfaces, resulting in poor cellular uptake.[29-31] Therefore, it is critical to design nanomaterials with the positive charges that can neutralize the negative charges and facilitate their interaction with the cellular surfaces.[29-33] Research has shown that positively charged carrier-DNA complexes promote cellular endocytosis of the particles by altering the structural properties and ion permeability of the cell membrane.[34] The overall positive charge is an essential requirement for the effective cellular association and subsequent internalization.[29,34]

In addition, it has been found that the surface charge of the particle also determines the colloidal stability of the dispersion and can be predicted by measuring the zeta potential of the system.[30-35] According to the conventional Derjaguin-Landau-Verwey-Overbeek (DLVO) theory, the interaction between two particles is the sum of the electrostatic repulsion and the van der Waals attraction [35]. Since the behavior of nano-scale materials in liquid medium is strongly dominated by the inter-particle forces [34], to achieve stable dispersion, one should consider generating like-charged surfaces that could provide sufficient electrostatic repulsion between the

particles to maintain their dispersion stability.[34] Dispersions with zeta potential below a critical value of 20-30 mV are relatively unstable and tend to aggregate easily.[35] Alternatively, a nanocarrier with an excess of positive charge can induce toxic effects by disrupting the cellular membrane.[34-36]

CHAPTER 2

LITERATURE REVIEW

2.1 NANODIAMONDS AS A NOVEL DRUG DELIEVRY SYSTEM (DDS)

In the search for advanced drug delivery systems (DDS) with the goals of improving bioavailability, preventing premature degradation, enhancing uptake, controlling the drug release rate and reducing side effects by only targeting the drug to the diseased site and target cells, nanodiamonds have emerged.[12] Numerous groups have exploited the surface chemistry of NDs and investigated their potential as drug delivery vehicles (DDVs).[13] Significant groundbreaking research applications in the use of NDs include: modulated release, drug delivery, biosensors and imaging probes.[12,13] NDs are excellent candidates towards the next generation of drug delivery systems, due to their inherent biocompatibility and optical properties which have been found extremely advantageous in the field of bioimaging and targeted delivery.[13] A number of experiments have shown that ND has the highest biocompatibility of all carbon-based nanomaterials including those of carbon blacks, multiwalled nanotubes, single-walled nanotubes and fullerenes.[14]

Nanodiamond is a term used to describe and identify a variety of structures that include diamond crystals found within interstellar dust and meteorites, diamond particles nucleated in gas phase or on the surface, and nanocrystalline films.[36-45] Nanodiamond is a novel carbon nanomaterial with useful properties including optical transparency, dimensional stability, chemical stability, and biocompatibility [35-37]. Diamond was synthesized in the 1950s from graphite using elevated temperature/pressure conditions[40]. In the next decade, chemical vapor

deposition at low pressures was used to synthesize polycrystalline films.[44] In the 1960s, research teams from DuPont De Nemour & Co, synthesized diamond from shock wave compression applied to carbon materials.[44-46] The resultant material was polycrystalline diamond with a grain size from 1 to 50 nm, and was used in high precision polishing applications.[46] A more efficient method to produce diamonds by detonation was perfected by Russian scientists through independent studies carried out during the 1960s.[47,48] Nanodiamonds (NDs) represent a new class of nanoparticle in the carbon family, with superb physical and chemical properties and tunable surface functionalization.[33]

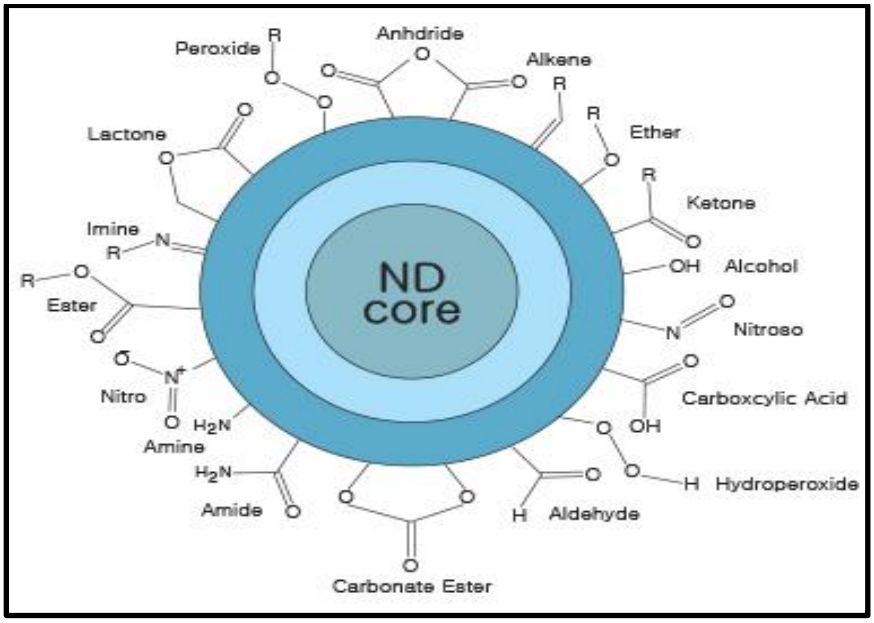

Figure 2.1 Surface functional groups commonly present on nanodiamond surface. [44]

Less than 1 micrometer, NDs are capable of being reduced to sizes between 4 to 5 nm. The small size of NDs yield high specific surface area and includes a chemically inert sp3 carbon material core. The surface of the material is rich in a wide variety of surface functional groups (Figure 2) following purification. As-produced, detonation diamond nanoparticles are

hydrophilic and can be chemically functionalized through a myriad of methods, ionic, physical adsorption, covalent, etc.

2.2 PRODUCTION OF NANODIAMONDS

Nanodiamonds are developed by two processes (detonation or phase transformation. Detonation of carbon-containing explosive materials (known as nanodiamond detonation) is a common method used to form abrasive nanodiamond materials.[41,44] Detonation nanodiamond (DND), is diamond that originates from a detonation. When an oxygen-deficient explosive mixture of TNT/RDX is detonated in a closed chamber, diamond particles with a diameter of ca. 5 nm are formed at the front of the detonation wave in the span of several microseconds.[45] A refinement process extracts various grades of these NDs also referred to as ultra-dispersed diamonds or 'UDD' that meet technical requirements for various applications including control of agglomeration and high suspension stability.[45-47] Phase transformation of the carbon precursors under high temperature and pressure after the micron-sized materials are disintegrated can also form nanodiamond materials.[47,48]

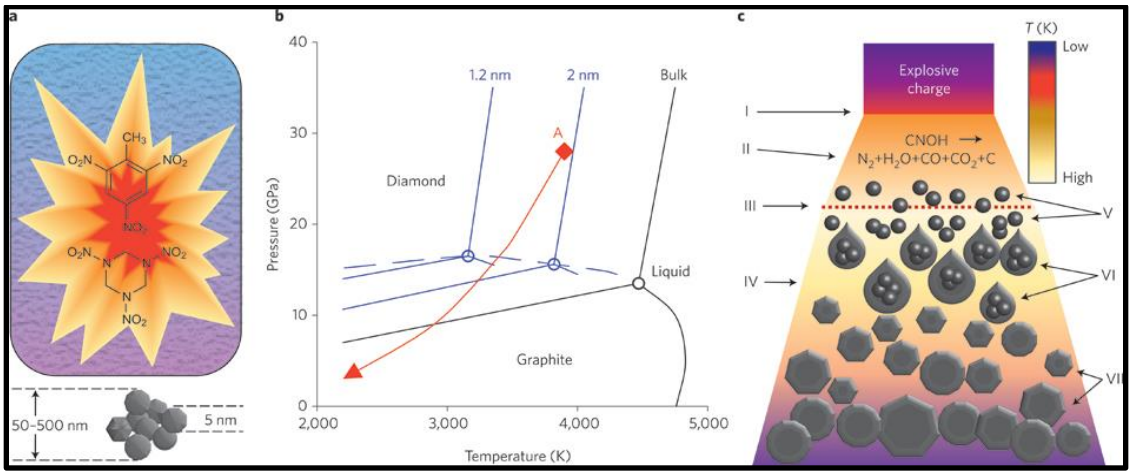

Figure 2.2 Production of Detonation Nanodiamonds (DNDs). [47]

2.3 STRUCTURE OF NANODIAMONDS

Elemental carbon has six electrons with an electronic configuration of 1s2 2s2 2p2 in its ground state.[49] The two electrons of the 1s orbital are core electrons, while the other four are valence electrons.[49] The sp2 hybridization of carbon atoms leads to the formation of the two-dimensional planar hexagonal structure of graphite.[49] In this type of arrangement, the central carbon is linked to three other carbon atoms by σ-bonds with the remaining electron of the p z orbital forming a delocalized cloud of π electrons over the graphitic structure.[49-51] The sp3 hybridization of carbon atoms forms a rigid diamond structure with tetrahedral symmetry, where all the four valence electrons of the carbon atom each form an σ bond with the neighboring carbon atoms.[49-51] The general lack of free electrons in the bulk structure of diamond accounts for their inertness[50]. However, the surface structure of the material is different from the bulk, due to the relaxation at the surface and the need to terminate the bonds.[50-52] Thus, the terminating structure on diamond surfaces involves univalent species such as H or OH or any terminating groups for both nano- and larger forms (synthetic and natural).[52]

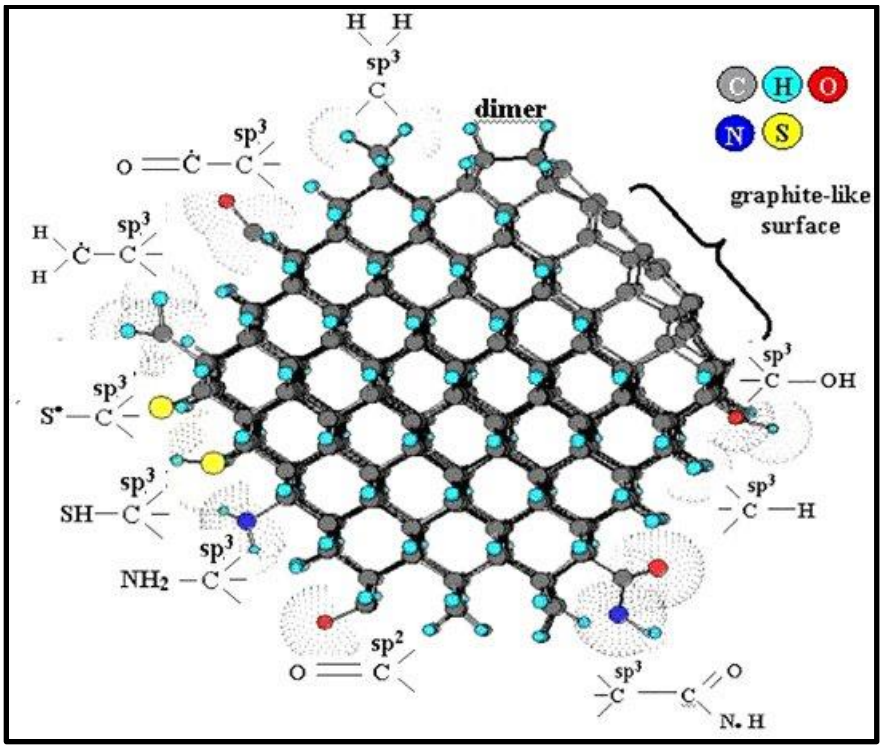

Figure 2.3 Nanodiamond internal core sp^3 structure and surface functional groups (sp^2, sp^3).[50]

Although the size, shape, and surface properties of NDs are determined by the nature of explosion and purification conditions, their basic structure follows a core and shell model.[33] The diamond carbon forms the inert core and the surface shell is partially comprised of graphitic structures. [30,45,46] In addition, a wide variety of functional groups such as carboxyl, hydroxyl, lactone, anhydride, ketone, and ether can be present on the surface of these ND particles.[45-47] The acid purification treatment increases the density of carboxylic and hydroxylic groups on the surface of NDs, resulting in their hydrophilicity.[50-52]

2.3.1 NITROGEN VACANCY CENTER (NV^{-1})

In contrast to other nanocarriers, such as nano-liposomes, gold nanoparticles, and nanotubes, nanodiamonds offer an attractive alternative in the field of biomedical research.[50-55] Particularly, due to their optical properties making these materials invaluable in the areas of bioimaging. Studies show that NDs are easily detected in vivo based upon optic research evaluated at specific wavelengths.[56] Applying a magnetic field, light or other sharp resonances in the intensity and wavelength of photoluminescence, it is applicable to view these materials in vivo.[53-55]

One of the major advantages of NDs is their inherent fluorescence at certain wavelengths due to nitrogen vacancy centers (NV^{-1}). Nitrogen vacancy is a term referring to the lone pair electrons because of a missing atom located outside its origin.[55-57] A NV^{-1} is a fluorescent point defect in diamond lattice that can respond by emitting wavelengths. Vaijayanthimala et al. described that some radiation-damaged NDs could emit durable and constant photoluminescence (red or green) that comes from the NV^{-1}.[57] NDs exhibit a major benefit to conventional probes, due to the NDs ability to display photoluminescence, low cytotoxicity without photobleaching, as well as a fluorescent lifetime of ~20ns, as opposed to conventional fluorescent probes which have a fluorescence lifetime of ~4ns; thereby enabling long term tracking within cells.[58,59] Figure 5, shown below, displays an image showing the fluorescent point defect that is responsible for the photoluminescence at a specific wavelength of energy.

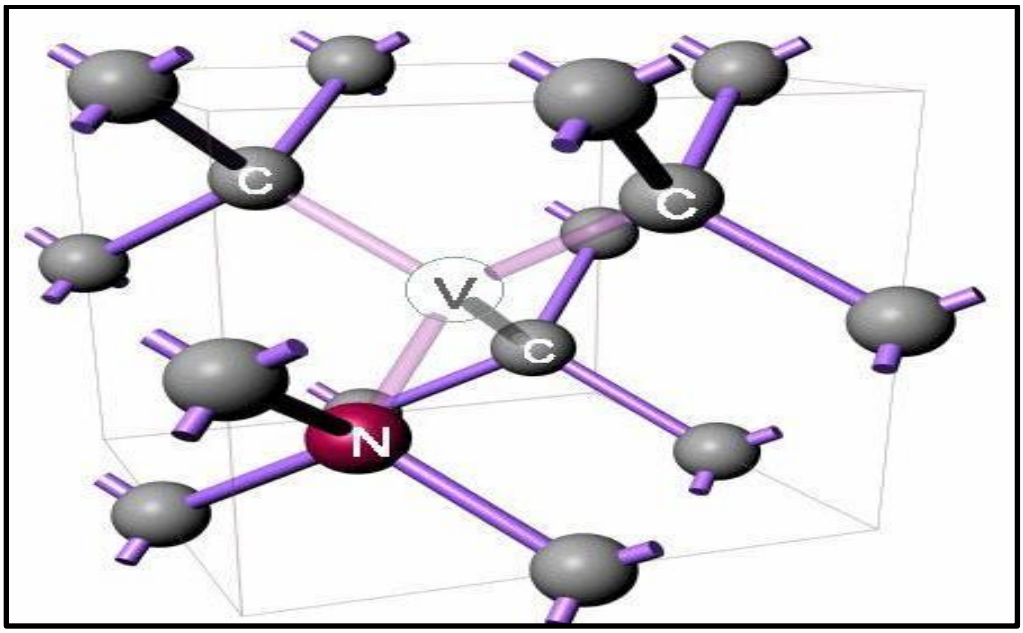

Figure 2.3.1.1 ND sp3 perfect crystal carbon pattern along with a nitrogen vacancy center capable of emitting a point fluorescent defect at a specific wavelength of energy.[60]

Within the nanodiamond structure, nitrogen exists as a trace impurity, along with Si and other certain types of transitions metals.[61] This is mostly due to the vacancies of the centers that yields the color that is given off once the nanodiamonds have been excited at the proper wavelength.[60-61] The photostability of nanodiamonds is often the most commonly utilized feature of the material along with the ease of conjugation to biomolecules that allow nanodiamonds to act as biosensors, biolabels, and biomarkers within the field of life science.[61] Another benefit of the color defects, is that it is embedded in the depths of the diamond matrix meaning that surface modification of the nanodiamonds does not directly affect the fluorescence of the nanodiamonds display.[61-63]

Based upon the presence or lack of nitrogen impurities in the crystal lattice structure, natural diamonds are classified as type I or type II, respectively.[63] The arrangement of nitrogen

impurities is used to sub-classify type I diamonds into type Ia and type Ib.[63] While type Ib contains atomically dispersed single substitutional nitrogen impurities (C-centers), type Ia diamonds comprise an aggregated form of nitrogen.[63] The latter are categorized further into type IaA, having two aggregated nitrogen atoms (A-center), type IaB, having platelets and four aggregated nitrogen atoms surrounding the nearest lattice vacancy (B-center), and type IaA/B, possessing the characteristics of both type IaA and type IaB.[63]

Synthetic diamonds manufactured under high-pressure high-temperature conditions are also known to contain a high amount of nitrogen in the form of impurities.[63-65] The natural diamonds have mainly aggregated nitrogen defects (type Ia), while synthetic high-pressure high-temperature diamonds are predominantly embellished with single substitutional nitrogen centers (type Ib).[63-65] Irradiation damage of type Ib diamond crystals creates intrinsic defects such as vacancies, which upon thermal annealing move towards nitrogen centers (N), and get trapped within to form nitrogen vacancy (N-V) color defect centers.[63]

Generally, irradiation of these diamond particles is carried out by high energy electron (~2-MeV) [63-65]or proton (~3-MeV) [63-65] beam using Van de Graaff or tandem particle accelerators, respectively. These sources generate vacancies but are difficult to install in usual pharmaceutical or biomedical laboratory settings due to their high cost, complicated setup, and safety issues.[63] Hence, to increase the feasibility of the production of fluorescent NDs on a wider scale, a moderate scale energy helium ion (40-keV) beam emanating from a radio frequency positive ion source was proposed.[63] Even though a much lower energy source was used in this irradiation process, none of the essential fluorescence spectral features were lost apart from a decrease in fluorescence intensity, when compared to the fluorescence spectra generated by 3-

MeV energy proton beam irradiated particles.[63] This method not only benefited the laboratories having ordinary infrastructure in producing fluorescent NDs, but also increased the yield of fluorescent NDs by creating a higher number of vacancies compared to electron and proton beam irradiated NDs [63-67].

Irradiated synthetic type Ib NDs, after 2 hours of annealing at 800°C, generated mainly two types of N-V defect centers, neutral nitrogen vacancy $(N\text{-}V)^0$ with zero phonon line at 575 nm and negatively charged nitrogen vacancy $(N\text{-}V)^-$ with zero phonon line at 638 nm.[64-68] Among all the color centers, $(N\text{-}V)^-$ dominate the fluorescence spectra of type Ib diamonds.[68] This defect center absorbs light photons at ~560 nm and fluoresces brightly at ~700 nm with a quantum efficiency close to 1.[66-68] Therefore, these centers offer characteristically bright red fluorescence to diamond particles upon excitation with green-yellow light [63] and hence have found applications for high-pressure high-temperature NDs in imaging studies.[63-65]

Extreme photostability of $(N\text{-}V)^-$ defect centers [65-68] provides a greater advantage to NDs to emerge as an excellent candidate for long-term cellular imaging over commonly used fluorophores. Red fluorescent NDs (100 nm) have been studied and were found to be stable with no observed photobleaching, upon continuous exposure to a 100 W lamp power for 480 minutes, whereas similarly sized red fluorescent polystyrene nanospheres photobleached within 30 minutes of photoexcitation.[69] In another instance, no photobleaching occurred in both 100 and 35 nm sized red fluorescent NDs when photoexcited with 8 kW/cm2 power density of light for 5 minutes.[68] On the other hand, under the same photoexcitation conditions, the fluorescence of Alexa Fluor 546 conjugated to DNA faded completely in 12 seconds.[69] Additionally, the fluorescence of red NDs was found to be significantly brighter than that emitted by Alexa Fluor

546 dye.[69] The evidence of photostability has also been determined for a 7 nm sized red fluorescent diamond nanocrystal that did not show any sign of photobleaching over a time period of 30 seconds.[69] In addition to resistance to photobleaching, the fluorescence of NDs (35 and 100 nm in size) was also found to be immune to photoblinking on a time scale of 1 ms.[70] Moreover, due to the deep location of $(N\text{-}V)^-$ centers in the lattice structure of NDs [70-73], the fluorescence remains unaffected by surface alterations, as evidenced by NDs functionalized with carboxylic acid [64], polylysine [65] and transferrin [71] groups.

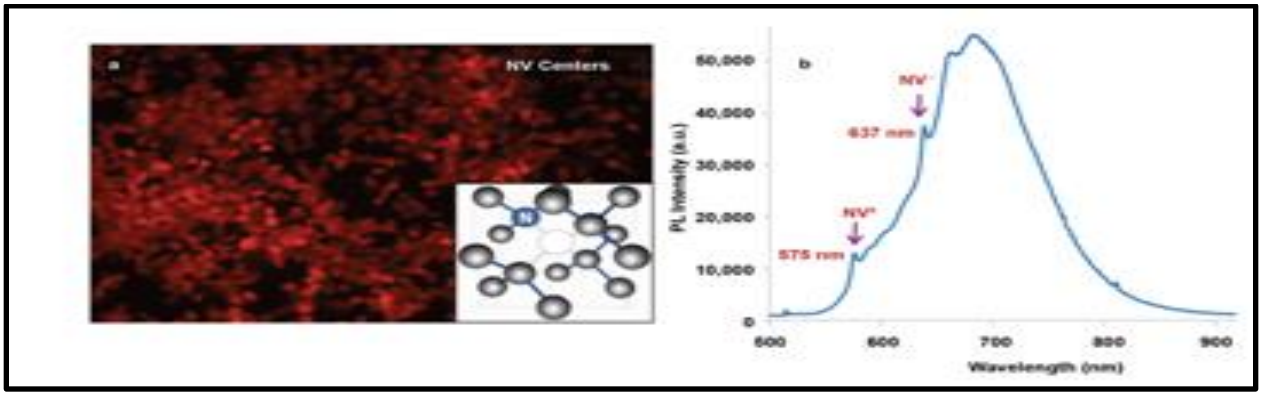

Figure 2.3.1.2 Fluorescent nanodiamond particles that contain nitrogen vacancy centers taken by an inverted fluorescent microscope, and the photoluminescence emission spectrum of the 100 nm ND that were dispersed into deionized water containing an excitation wavelength of 532 nm while containing a red/near-infrared emission between the wavelengths of 635-800 nm.[57]

As previously noted, the average fluorescence lifetime of NDs is ~17 ns, which is considerably longer than the lifetime of fluorescent organic dyes (<5 ns) and most of the cellular endogenous fluorophores (<6 ns).[65-70] Table 1 lists the advantages of using red fluorescent NDs as a fluorescent tag for *in vitro* or *in vivo* tracking applications. As of result of these

characteristics, the intrinsic photostability of NDs opens avenues for carrying out chemical modification of their surface for specific imaging applications.

Table 2.3.1 Properties and Advantages of Nanodiamonds

Properties	**Advantages**
High quantum efficiency	Bright fluorescence
Photostability over longer time periods	Long term tracking of nanodiamonds in cells
Emission wavelength >690nm	Sharp contrast imaging of nanodiamonds
Longer fluorescence lifetime	High contract imaging of nanodiamonds
Deeper location of nitrogen vacancy centers	No alteration in fluorescence due to surface modification

2.3.2 NVN

Like the N-V defect centers of type Ib synthetic diamonds, the nitrogen-vacancy-nitrogen (N-V-N) or H3 defects centers[50] in natural type Ia diamond nanocrystals can be created by irradiating them with a high energy (3-MeV) proton or a medium energy (40-keV) helium ion beam followed by annealing at 800°C.[52] H3 defect centers have a zero phonon line at 503 nm, with absorption and fluorescence emission at 470 and 530 nm, respectively.[52] Therefore, type Ia NDs with H3 centers are known as green fluorescent NDs.[52]

Other than the natural and high-pressure high-temperature NDs containing nitrogen impurities, researchers are also trying to understand the fluorescence characteristics of detonation NDs. However, considering the actual composition of the explosive mixture (~20 mass% of nitrogen) used to synthesize these particles, they might contain a high concentration of nitrogen [50-55] either in their core structure or in the form of surface defects. At first, these nanoparticles were suggested to be devoid of C-centers and were believed to be unsuitable for imaging applications.[51] The absence of zero phonon lines corresponding to the nitrogen vacancy centers in irradiated and annealed detonation NDs suggested structural defects to be the origin of their fluorescence.[51-53] Z-contrast scanning transmission microscopy, high-resolution transmission electron microscopy and electron energy loss spectroscopy identified nitrogen in the core structure of detonation NDs.[55]

Recently, Vlasov et al detected stable (N-V) color centers in detonation NDs having a size greater 30 nm after their irradiation and thermal annealing treatment.[54-57] While the occurrence of (N-V) color centers in the bulk structure of detonation NDs of less than 10 nm size has been questioned in various studies [55-60], Smith et al showed the presence of these centers in single-digit-sized irradiation damaged and annealed NDs.[55] Moreover, (N-V) color centers have also been discovered in non-irradiated, 5 nm sized detonation NDs.[53] The NDs synthesized by detonation technique are shown to possess up to 3 at.% of nitrogen impurities.[51-55]

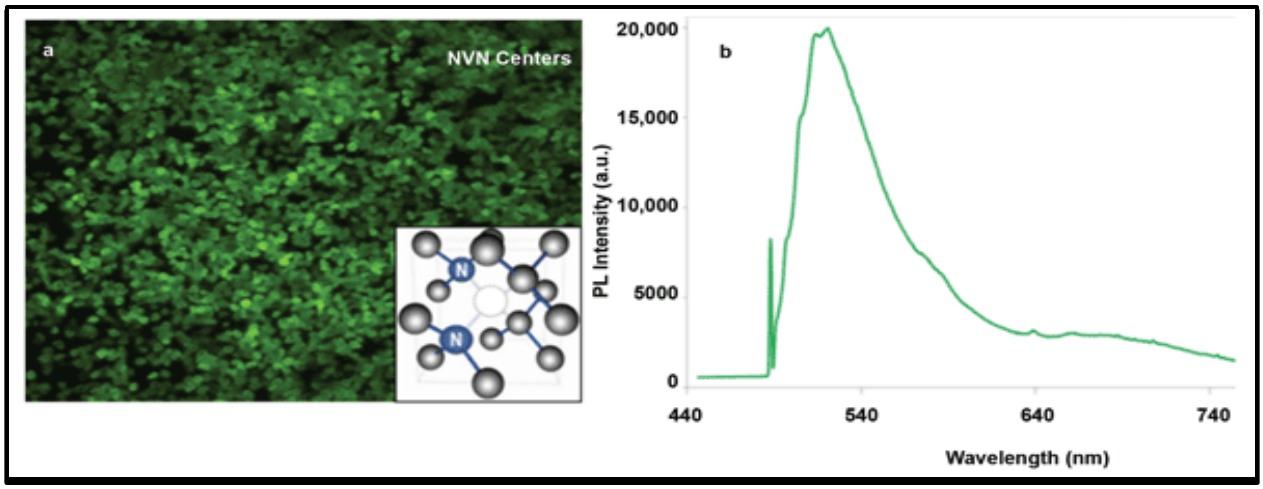

Figure 2.3.2 Fluorescent nanodiamond particles that contain nitrogen vacancy nitrogen (NVN) centers (H3 centers) taken by the inverted fluorescent microscope and the photoluminescence emission spectrum of 70 nm NDs. NDs were dispersed in a 1mg/L solution of water and they contain an excitation spectra of 432 nm.[57]

2.4 AGGREGATION PHENOMENA

Nanoparticles in dry powder state tend to form agglomerates; thereby reducing their high surface energy.[11] This property represents a significant obstacle for certain applications. Detonation nanodiamond particles are particularly known to form agglomerates that cannot be destroyed by traditional means such as sonication, milling, etc.[9-12] The rich surface chemistry of ND generally explains this. The presence of diverse functional groups on ND surface, such as carboxyl, hydroxyl, lactone, etc., may result in formation of multiple hydrogen and even covalent bonds between the adjacent ND particles. Thus, strong agglomeration severely limits potential of NDs in many applications.

Extreme conditions caused from the surface functional groups reaction causes formation of strong inter-particle covalent bonding otherwise known as graphitic cells.[17] As the surface area to volume ratio of the particles increases with the decrease in the size, the Van der Waals forces along with electrostatic interactions and chemical bonding dominate [17], leading to a significant aggregation of nanoparticles.[15-17] Systemic administration of aggregating nanoparticles can result in the blockage of the blood flow in the blood vessels.[10-15] Aggregated particles could also accumulate in various organs of the body, leading to severe consequences such as stroke.[14] Furthermore, agglomeration can also initiate an immune response.[13-15] As evidence, aggregated carbon nanotubes have shown higher *in vitro* toxic effects compared to their dispersed state [21]. Aggregation of nanoparticles has also been shown to adversely affect cellular interactions ultimately influencing cellular uptake.[13,15-17]

Maintaining nano-scale particle size necessitates the use of mechanochemical treatment that not only leads to disaggregation but also prevents the re-aggregation of particles.[72-75]Mechanical treatment such as sonication can break the aggregates without affecting the surface properties of particles, and then chemical functionalization can sterically and/or electrostatically stabilize the dispersion.[72] Therefore, mechanochemical treatment has a potential to reduce the size of aggregated particles and maintain their dispersion stability.

2.4.1 CURRENT METHODS OF DEAGGREGATION

The dispersibility of nanodiamonds in aqueous solutions is an extremely important criterion for biological applications. Traditional techniques of disaggregation to assist in the dispersion of nanodiamonds have consisted of milling, emulsification, and low power sonication.[75-78] All of which have been ineffective in breaking down the tightly bound core

aggregates of NDs to less than 10 nm.[75] To achieve primary-sized NDs, milling has been studied using 100-μm silica beads.[75] Single-digit-sized NDs were obtained after an hour of sonication of the diluted milled suspension and the stability of the resulting aqueous colloid was maintained for a year.[75] However, reconstitution with water after drying the nanodispersion resulted in reaggregation with 2.3 μm size aggregates.[75] Bead assisted sonic disintegration using zirconia beads has also gained interest for breaking the ND aggregates into single-digit-sized particles.[76] This mechanical technique involves the combination of shear forces induced by beads with their acceleration during cavitation created by intense ultrasonic waves.[76] These primary sized NDs exhibited very good colloidal stability in polar solvents such as water and DMSO.[76] However, contamination from the beads [75] and from the sonicator itself have proved to an obstacle for these technologies.[75-78]

Mechanochemical treatment, which involves the breaking of ND aggregates by mechanical energy using surfactants was also explored to achieve stable dispersions with a noticeable size reduction.[75-79] However, a primary dispersed particle size of less than 10 nm was not achieved.[79] Ultracentrifugation, a contamination-free procedure, resulted in 4 nm size NDs that formed a stable colloidal dispersion in water[79-84] but suffered from low yields of single- ND particles. Hence there is still a need for development of easy, feasible, contamination-free techniques that can result in disaggregation of NDs at the laboratory scale.

In 2005, Osawa et al. achieved nanodiamond disintegration into primary particles through stirred media milling.[85] Nanodiamond were milled using 30 μm diameter zirconia beads in the presence of water in a vertical stirred mill for three hours. The beads were separated by filtration, and the slurry was diluted and sonicated to obtain a colloidal solution of disaggregated

nanodiamond.[82-85] The author proposes that the disaggregation may be caused by a shearing action of beads in the turbulent flow of slurry rather than head-on collisions between beads and nanodiamond aggregates.[85] Wet media milling often results in contamination of nanodiamond slurries with fragments of zirconia beads, which are difficult to remove by filtration or centrifugation techniques. Osawa et al. improved upon stirred media milling and reported the dispersion behavior of nanodiamond in organic solvents. [85] It was established that smaller zirconia beads (20 μm) resulted in improved efficiency of the milling process. However, the procedure breaks down the components of the milling apparatus. Furthermore, it has been observed that higher peripheral speed and longer milling time increase levels of zirconia contamination[81]. The group proposed using high power sonication of nanodiamond aggregates along with zirconia beads to disintegrate aggregates.[81]

In this work, a simple and efficient deagglomeration technique to mill nanodiamond into primary particles using sodium chloride as milling media is explored. The hardness of the dry media renders it capable of decreasing the size of nanodiamond agglomerates.[82] Furthermore, the media surrounds the milled nanodiamond and isolates individual particles, preventing reagglomeration.[82] The media can be easily removed after milling leaving no contamination in nanodiamond.

2.4.2 SALT ASSISTED BALL MILLING

Nanodiamond disaggregation is a notoriously challenging task. Existing protocols, as previously discussed, make use of zirconia microbeads propelled by mechanical energy or cavitation[79-81]. These materials are expensive and leave behind difficult-to-remove debris of zirconia. Salt assisted ball milling is a facile, inexpensive, and contaminant-free technique of

deaggregation[82]. The technique utilizes salt slurry in contrast to current disaggregation techniques, which introduce zirconia contaminants. The nanodiamonds produced by this technique have no toxic or difficult-to-remove impurities and are well-suited to produce nanodiamonds for numerous applications.

2.5 CHITOSAN

Chitosan (CS) is a natural, linear polysaccharide polymer composed of glucosamine and N-acetyl glucosamine units linked by β (1-4) glycosidic bonds.[87-89] Chitosan is produced from the deacetylation of chitin, a polysaccharide most often present in crustacean shells.[87-89] Chitosan is biocompatible, biodegradable, hydrophilic, non-toxic and displays antimicrobial properties all of which are important in biomedical applications.[86-89]

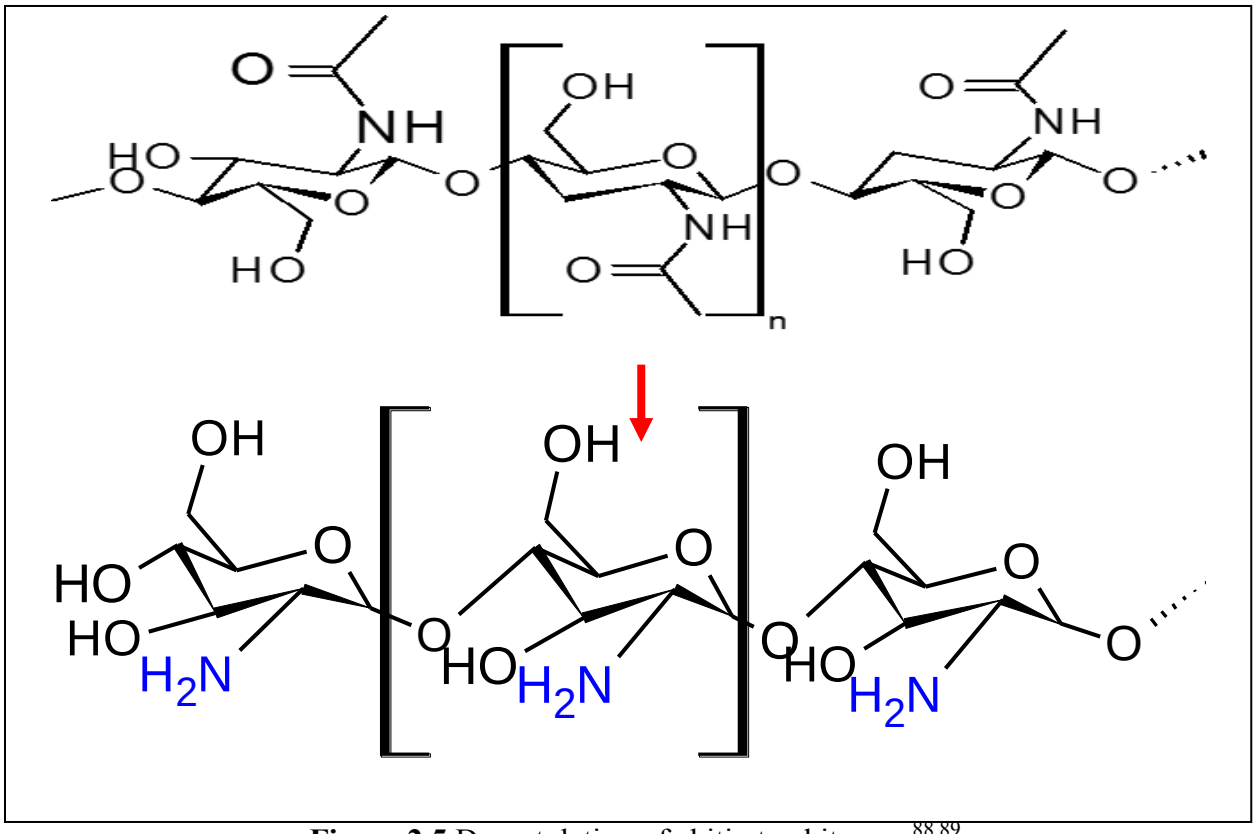

Figure 2.5 Deacetylation of chitin to chitosan. [88,89]

2.6 SURFACE MODIFICATION OF NANODIAMONDS

The features of nanodiamonds such as the nano-size, the larger surface area, and potential for purification with oxidizing agents, make NDs a viable candidate for surface functionalization.[90-93] The functionalization of NDs is critical in making DNDs suitable for commercial applications. Figure 9 summarizes approaches used in the past to introduce various functionalities on the surface of NDs.[82] One of the earliest modifications of the ND surface involved the generation of surface radicals, which then acted as substrates for synthesizing carboxylic[78] and dicarboxylic acid[79] functionalized NDs. For a high surface loading, it is essential to achieve surface uniformity. Reactions with hydrogen [78,79], chlorine [80], and fluorine[81] have been explored to attain surface homogeneity as well as reactivity enhancement. The surfaces of chlorinated NDs were further modified with hydroxyl, amine, and carbon fluoride groups.[80] Finally, reactions of NDs with alkyl lithium, ethylenediamine and glycine ethyl ester hydrochloride generated alkyl, amino and glycine substituted NDs, respectively.[81]

Pristi et al. devised a new method for the functionalization of detonation nanodiamonds (DNDs), based on surface modification with phosphonic dichloride derivatives. DNDs were first modified by phenylphosphonic dichloride, and the grafting modes and hydrolytic stability under neutral conditions were investigated using ^{1}H, ^{13}C, and ^{31}P solid state NMR spectroscopy, Fourier transform infrared spectroscopy, as well as elemental analysis. Then, to illustrate the possibilities offered by this method, DNDs functionalized by mesityl imidazolium groups were obtained by post-modification of DNDs modified by 12-bromododecylphosphonic dichloride. The oxidative thermal stability of the functionalized DNDs was greatly enhanced and provided promising results for application in nanocomposite materials.

Mona et al. reported modifications in structural and surface properties of carboxylated nanodiamond (cND) due to thermal annealing from 150 °C to 900 °C and gas treatments (hydrogen/argon) at 650 °C. Significant enhancement of photoluminescence intensity and transformation of the shape of luminescence band were observed for gas treated cNDs and for thermally annealed NDs at 850 °C. FTIR results showed notable change in absorption frequency of carboxyl group (C=O). The results from these findings indicate modifying NDs surface improves the luminescence of ND, justifying their role in bio-labeling.

Surface functionalization has also emerged as a novel treatment for reducing aggregate sizes of NDs. Functionalization with long alkyl chains reduced the particle size from 15-μm to 150-450 nm.[82] The long alkyl chain-modified NDs showed an enhanced dispersibility in organic solvents compared to their pristine form.[82] Similarly, surface modification with fluorine contributed to size reduction from 1930 to 160 nm.[81] A noticeable size reduction of the micrometer-sized pristine NDs to ~ 50-nm was also achieved upon reduction of the ND surface groups with borane, which, after being grafted with alkyl silane, were used to synthesize biotinylated NDs with a surface loading of 1.45 mmol/g.[82] Nanodiamond functionalization using biomacromolecules has also been investigated using proteins, hormones, enzymes, DNA, or drugs attached via electrostatic interaction or covalent bonding.[82-84]

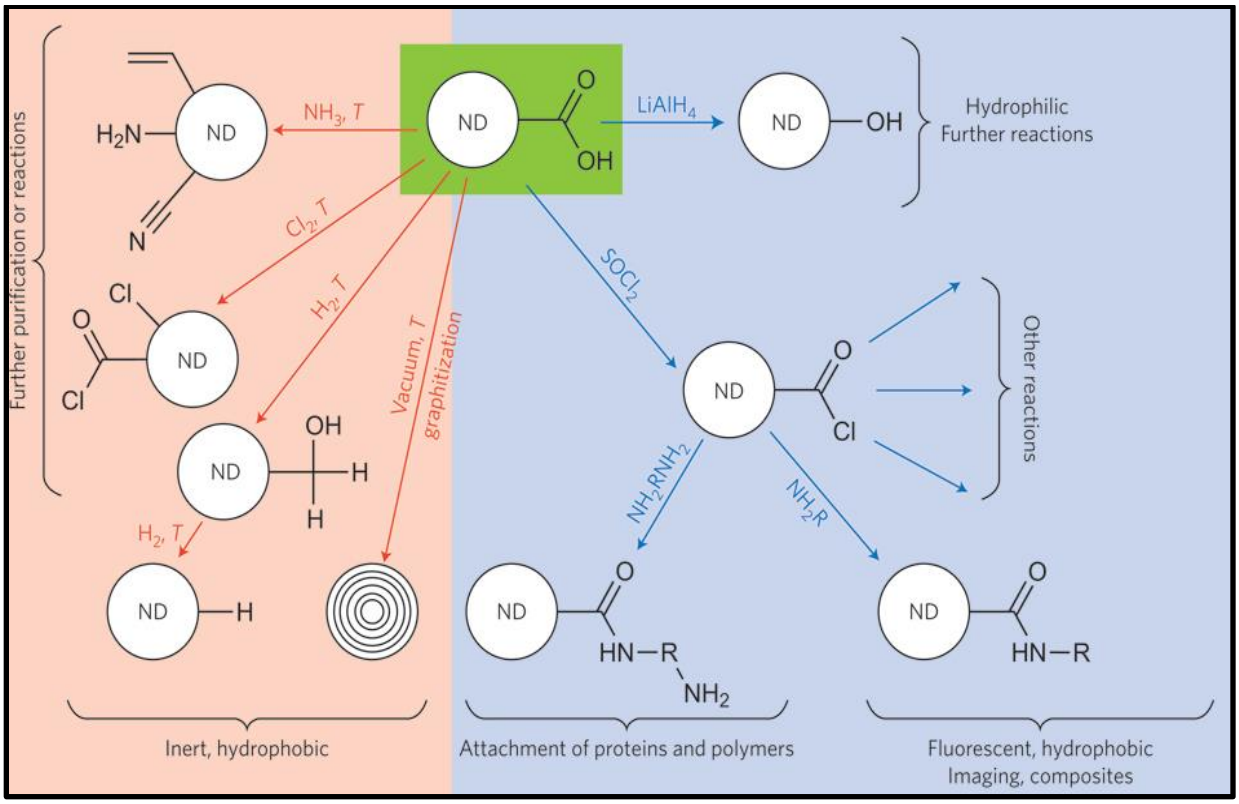

Figure 2.6 Distinct ways to modify the Surfaces of the Nanodiamond Functional Groups.[82]

2.7 BIOCOMPATIBILITY OF NANODIAMONDS

The intrinsic biocompatibility of detonation NDs has been supported by the results of several studies [90-92], however, some studies have refuted this claim by arguing that NDs can induce toxic responses under certain conditions.[90-92] In 2016, Wasowicz studied the interactions of modified nanodiamond particles in vitro with human blood. Modifications performed on the nanodiamond particles included oxygenation and hydrogenation upon chemical vapor deposition (CVD) plasma treatment. NDs were incubated in whole human blood for different time intervals. The morphology of red blood cells was assessed along with spectral measurements. These results showed that no more than 3% of cells were affected by the nanodiamonds and that NDs were

biocompatible with human blood. This work formed the basis for the development of nanoscale biomarkers.

Numerous studies have demonstrated that the toxicity of NDs can vary depending upon their surface chemistry [97-99], type of cell line [98-107] and the treatment medium [98] composition. The amine terminated NDs exhibited a higher toxicity (~22% cell death) than hydroxyl (~11%) and carboxyl group (~7%) terminated NDs in human kidney cells at a concentration of up to 200 μg/mL.[99] The carboxylated NDs did not show any significant toxic effects in mice [99], but induced DNA damage in stem cells [99], although to a lesser extent than that occurred with multi-walled carbon nanotubes. In another instance, a 100% viability of human cervical cancer (Hela) cells was observed after incubating them with 0.1-100 μg/mL NDs in a medium containing serum for 24 hours.[100-102] In the absence of serum, this viability dropped dramatically to almost 0% within 6 hours of dosage with 50 μg/mL NDs.[103]

Another study found that nanoparticles could adsorb the essential micronutrients from the medium and hence indirectly produce cytotoxic effects by depleting the cellular structures of essential nutrients.[103] In this work, NDs did not show significant toxicity, even when incubated with cells in medium lacking serum.[103] In addition to cellular studies, some *in vivo* studies have also been conducted to evaluate the toxicity of NDs. Intravenous administration of 125 mg of modified NDs did not cause any death in rabbits.[103] Neither the red blood cell count nor the hemoglobin level of rabbits decreased after 15 minutes of administering 50 mg of modified NDs, intravenously.[103] However, after 48 hours of injection, the levels of biochemical molecules altered significantly.[103]

In another study, an oral administration of 0.002 to 0.05 wt.% of ND hydrosols to mice, in place of water, for 6 months showed no significant abnormalities in growth or organs weight.[104] The NDs exhibited low toxicity and were cleared from the lungs after 90 days in mice.[104] Furthermore, the clearance of XenoFluor 750 labeled NDs from all the body organs of mice occurred in 3 to 10 days after injection at a dose of 120 μg.[104]

In summary, NDs have shown biocompatibility in various cell lines and some animal models with minimal or no cytotoxicity, demonstrating their potential for biomedical applications. However, it is well documented that the purity, surface chemistry and dimensions of particles should be considered carefully. More comprehensive and long term animal studies need to be conducted to verify the safety of NDs.

2.7.1 INTRACELLULAR UPTAKE OF NANODIAMONDS

Several studies have demonstrated the ability of NDs to internalize into cells [105-109]. Faklaris et al demonstrated that NDs having an average size of 46 nm were transported into Hela cells after 2 hours of incubation. [106] In addition, 100 nm sized NDs were also found to be internalized by cancer and stem cells after 4 hours of incubation [106]. The intracellular presence of the NDs suggests that these nanoparticles have a potential to be employed for the intracellular delivery of therapeutic molecules. This intracellular transport of NDs into cells has been shown to be dependent upon their surface characteristics [106-110], incubation time, and other physiochemical parameters such as size, shape, aggregation etc. Intracellular delivery of NDs opens perspectives for their use as delivery agents for chemotherapeutic agents.[112-124]

2.7.2 NANODIAMONDS IN THE DELIVERY OF DRUGS

In 2007, the suitability of NDs to act as a delivery agent of doxorubicin hydrochloride (DOX) was evaluated.[51,53,112] The investigation was based on the rationale that the surface carboxylic and hydroxylic groups of detonations NDs can interact efficiently with the amine groups of DOX via ionic forces when dispersed in aqueous medium.[121] The surface loading of DOX on NDs increased from 0.5 to 10 wt.% upon addition of 1% sodium chloride solution to their aqueous dispersion, and the removal of salt favored the release of DOX.[121] NDs loaded with DOX were suggested to assemble in the form of loose clusters, such that a certain amount of DOX adsorbed on the NDs surface resides within the cavity of the complex.[121] This strategy of drug entrapment in loose aggregates of NDs could provide an advantage by minimizing the systemic adverse effects of the naked DOX.[121] Thus, ND-based delivery systems could overcome the limitation to the use of high concentrations of chemotherapeutic drugs [79] in cancer treatments. In addition, the lower cytotoxicity of the ND-DOX composite in mice compared to bare DOX in a 48-hour period could be beneficial in sustained drug release.[121]

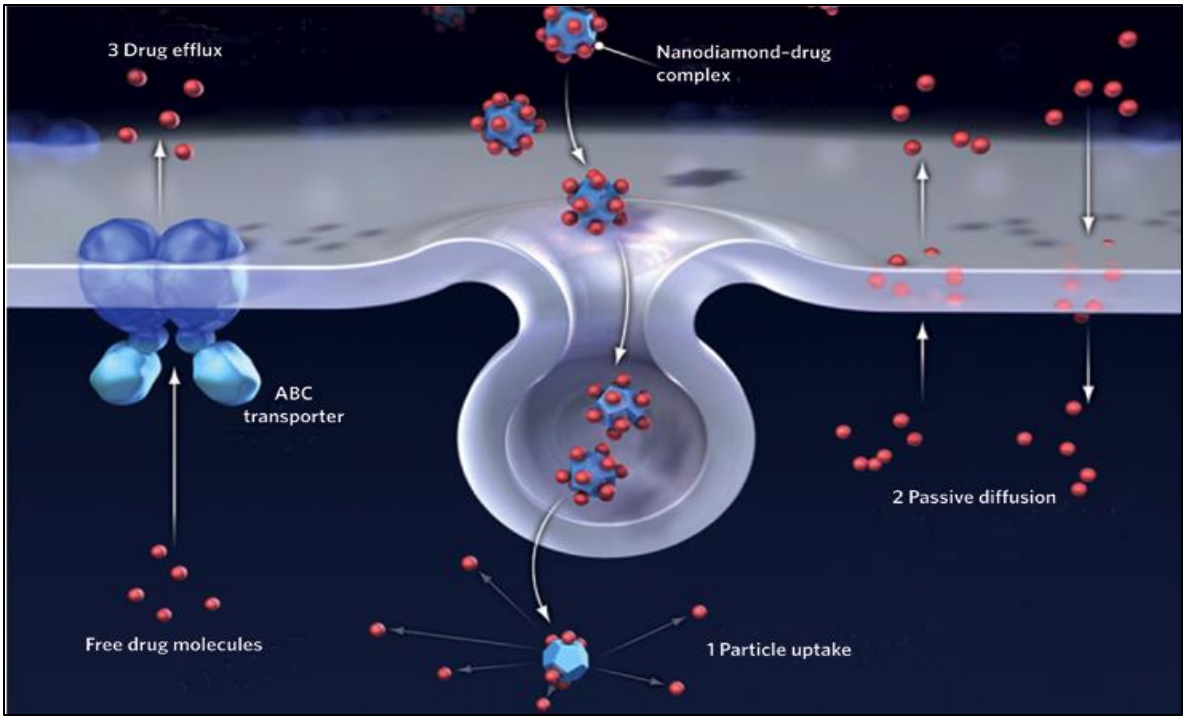

Figure 2.7.2.1 Transport of the Nanodiamond-drug complex through particle uptake releasing drug for an effective treatment.[82]

Another study, published in 2010, proposed NDs as efficient multifunctional delivery agents for the chemotherapeutic drug, 10-hydroxycamptothecin (HCPT).[69,112] Like the previous study by Huang et al [69,92], NDs could adsorb the drug onto their surfaces via simple physical forces.[69,92] However, in this case, the surface loading of HCPT was considerably enhanced to 50 wt.% from 0.4 wt.% with an increase in pH of the HCPT solution from 7 to 8.2, rather than by means of salination.[69] NDs released HCPT slowly into the PBS medium over a period of 5 days, with only 38% release observed in the first 24 hours.[69] In addition, the ND-HCPT complex showed almost 2.5 times higher cytotoxicity in Hela cells compared to the chemotherapeutic activity of HCPT alone, credited to the ND triggered intracellular delivery of HCPT.[69] Bovine serum albumin adsorbed on the surface of NDs rapidly (< 1 hour) while HCPT showed a gradual

adsorption (> 120 hours).[69] A model was proposed suggesting porous clusters of NDs in which small molecules diffused inside the clusters and the large molecules adsorb only on the outer surface of NDs.[69] Hence, NDs have been found to facilitate the intracellular delivery of both small molecule drugs and large therapeutic biomolecules.

Detonation NDs have also been utilized to increase the aqueous dispersibility of hydrophobic drugs. Poorly-water soluble chemotherapeutic drugs such as, Purvalanol A with therapeutic activity against liver cancer,[69,69,80] and 4-hydroxytamoxifen with a high potential to treat breast cancer,[69] are soluble in the polar, organic solvents DMSO and ethanol, respectively.[69] The use of non-aqueous solvents limits the administration of these formulations. However, when formulated with NDs, the aqueous dispersibility of Purvalanol A and 4-hydroxytamoxifen enhanced markedly.[64,69] By adsorbing the drug on their surfaces, NDs considerably reduced particle size and increased the zeta potential of these drugs in water, promoting their dispersibility and, potentially, cellular uptake.[106-115] Like the previous studies, NDs preserved the therapeutic activity of the drugs. These findings suggest that NDs could play an important role in designing nano formulations of water insoluble drugs.

Recently, it was discovered that the absorption of the sodium ions, helps to draw a deeper understanding on ND release and cellular response, Zhu et. al.[116,122] In this work, metal ions were attached to the nanodiamond aggregates and released into the living cell triggering cytotoxicity.[116] Zhu et al investigated the biomolecular interactions to elucidate the potential of nanoparticle-ions.[116]

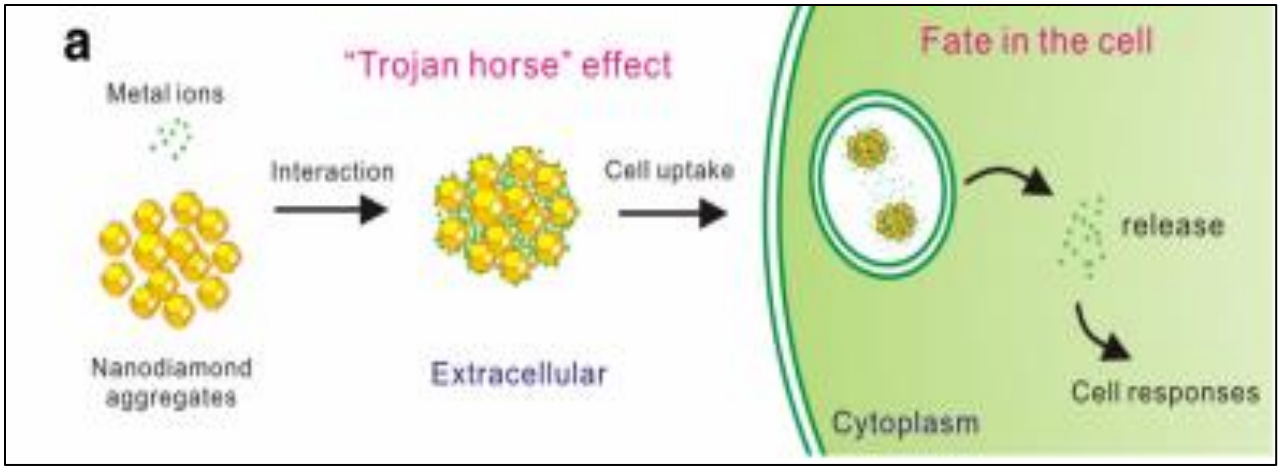

Figure 2.7.2.2 The adsorption of metal ions attached to NDs as composites released into the living cell.[116]

In this work, nanodiamonds were exposed to Cu^{2+}, Ni^{2+}, Cd^{2+}, and Cr^{3t} to assess toxicity.[116] plasma mass spectrometry determined the mean absorption of each transitional metal. Cu^{2+} was determined as the most effective metal in the assessment of cytotoxicity and cellular response. From these findings, Zhu utilized cell viability assessments of human bronchial epithelial (BEAS-2B) cells and human keratinocyte cells (HaCaT) to further explore cellular response.[116]

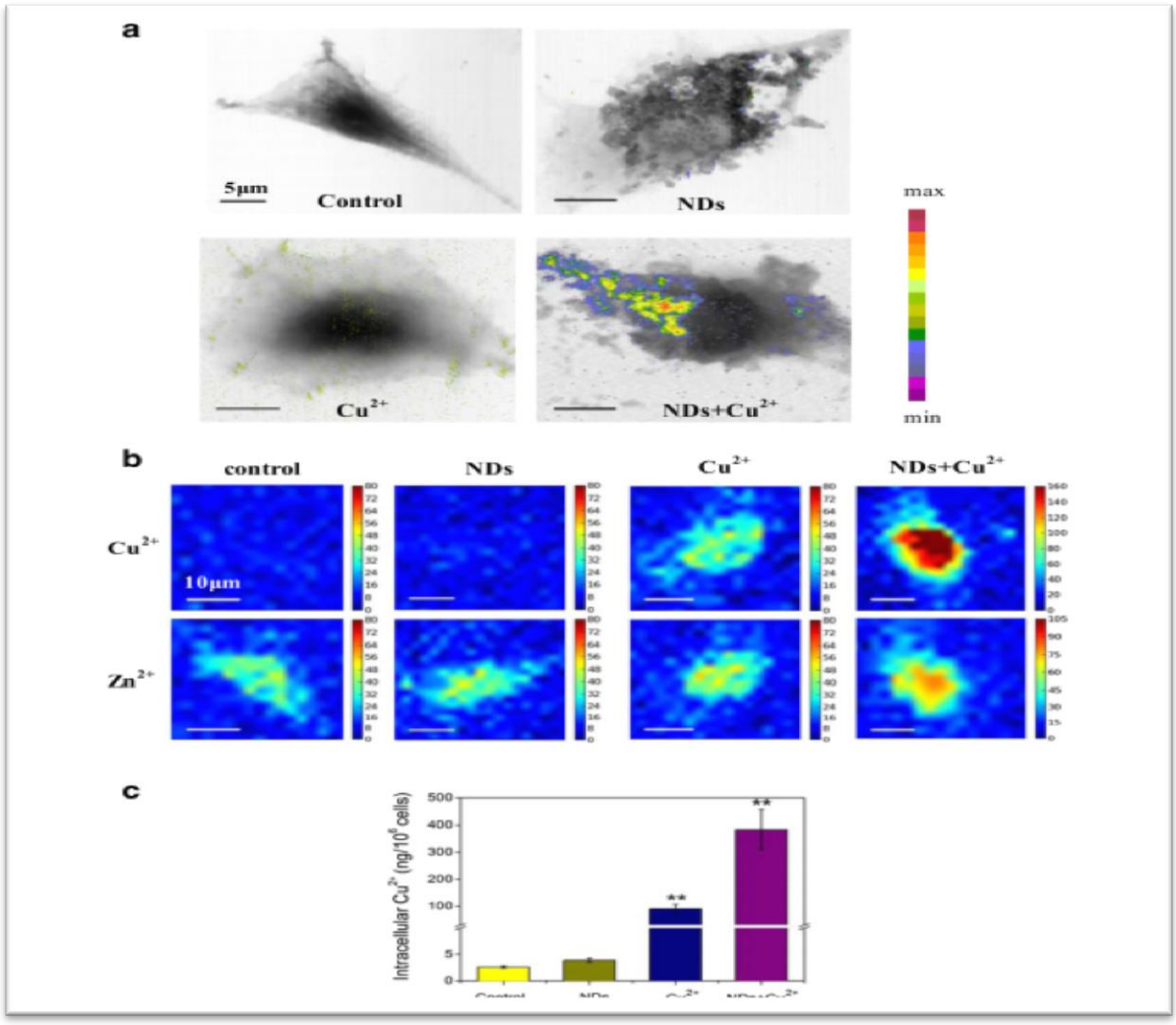

Figure 2.7.2.3 An interaction between the ND and Cu^{2+} complex to determine their internalization. A figure displaying the distribution of copper of a control cell (L929) (Top left) Cells after the incubation process (top right), cells after their incubation in NDS (Bottom right) copper (bottom left) via scanning transmission X-ray microscopy. b: Comparison of copper vs. zinc distribution using MicroXRF. c: ICP-MS intracellular measurement of copper with and without NDs.[116]

The efficacy of NDs to deliver chemotherapeutic drugs was examined recently in animal models for the first time. In addition to generalized toxicity, large particle size and poor water solubility, chemotherapeutic drugs also suffer from acquired and chemo resistance of tumor cells [115]. This challenge could be addressed by using a delivery system that not only enhances the uptake of the chemotherapeutic drugs but also retains them in the cancer cells for a longer period.[74,117] The study revealed that DOX bound to the ND surface was significantly more toxic towards DOX resistant mice compared to bare DOX.[74] The high chemotherapeutic efficacy of the ND-DOX composite was attributed to ND mediated DOX retention in tumor cells as determined by fluorescence microscopy and quantitative analysis.[74] Moreover, long term treatment showed superiority of the DOX bound to ND over the bare DOX in preventing tumor growth.[74] NDs not only circumvented the premature efflux of DOX from tumor cells, but also improved the adverse effects of naked DOX, by significantly reducing death.[74] In addition, NDs increased the circulation half time of DOX from 0.83 to 8.43 hours.[74]

In summary, the finding of Dean Ho *et. al* proved nanodiamonds (1) to be less expensive to produce in copious quantities. The nanodiamonds lattice structure possesses electrical charges, which allows tumor drugs to attach to nanodiamond surfaces developing a more effective method for drug delivery as shown in Figure 10. The nanodiamonds capability to be loaded with both drug and agent help target the cancer cells; thereby reducing the cytotoxicity of drugs.

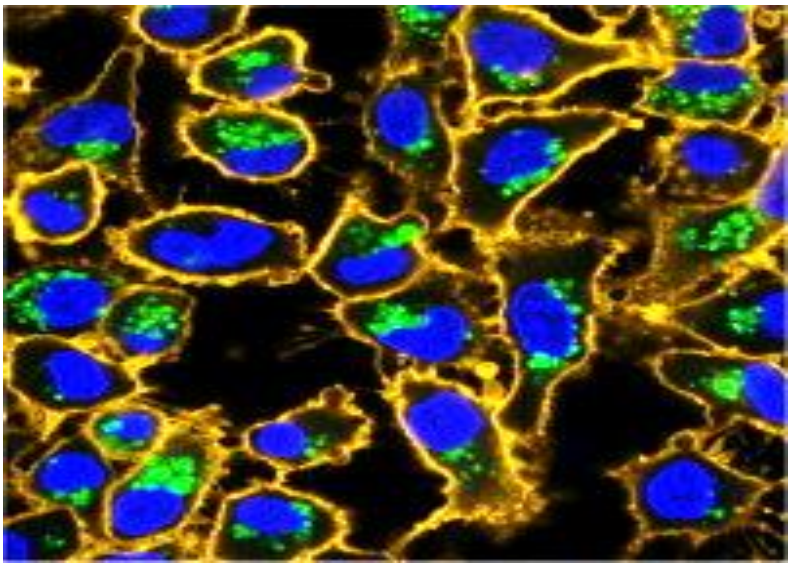

Figure 2.7.2.4 A Confocal Microscope image displaying the fluorescent NDs acting as cellular Biomarkers and drug transporters.[124]

The formulation of chemotherapeutic drugs with NDs improves the pharmaceutical properties of the agents by high surface loading, improved aqueous dispersibility, sustained release, and enhanced retention in chemo-resistant cells. These properties are due to the hydrophilic functional group-enriched surface, large surface to volume ratio, ability to form complexes, improved cellular delivery, and biocompatibility of the NDs.[115-124] Hence, NDs are suitable platforms to build nanoparticles for overcoming some of the major deficiencies of the chemotherapeutic drugs. In addition to small molecules, NDs have also shown potential as delivery agents for protein, DNA, and RNA. To date, there are limited studies regarding the applications of NDs as drug delivery agents. More studies are needed to verify their potential and to translate their use as a delivery agent into clinical applications. Chow et al., presents a study to demonstrate NDs failure to display any inflammatory responses in figure 2.7.2.5, as well as NDs ability to demonstrate an apoptotic effect as these nanomaterials increase the exposure of DOX

to the liver cells than the DOX does solely, furthermore, demonstrating NDs potential in biomedicine.[121]

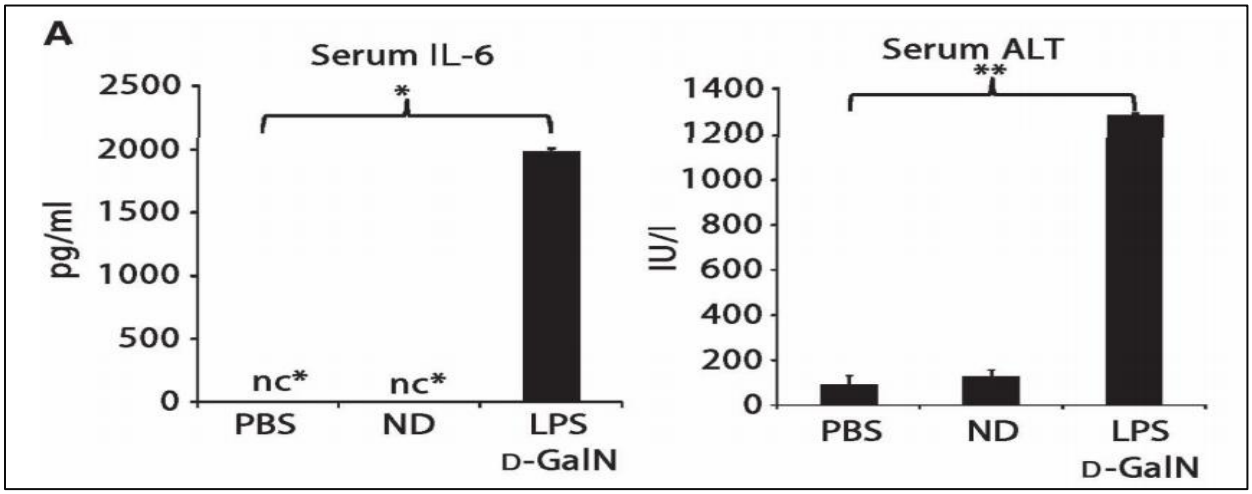

Figure 2.7.2.5 Graphs demonstrating NDs failure to induce elevated sera interleukin-6 (IL-6) concentrations, which is indicative of a lack of systemic inflammatory responses. ~LPS(Lipopolysaccharides). [121]

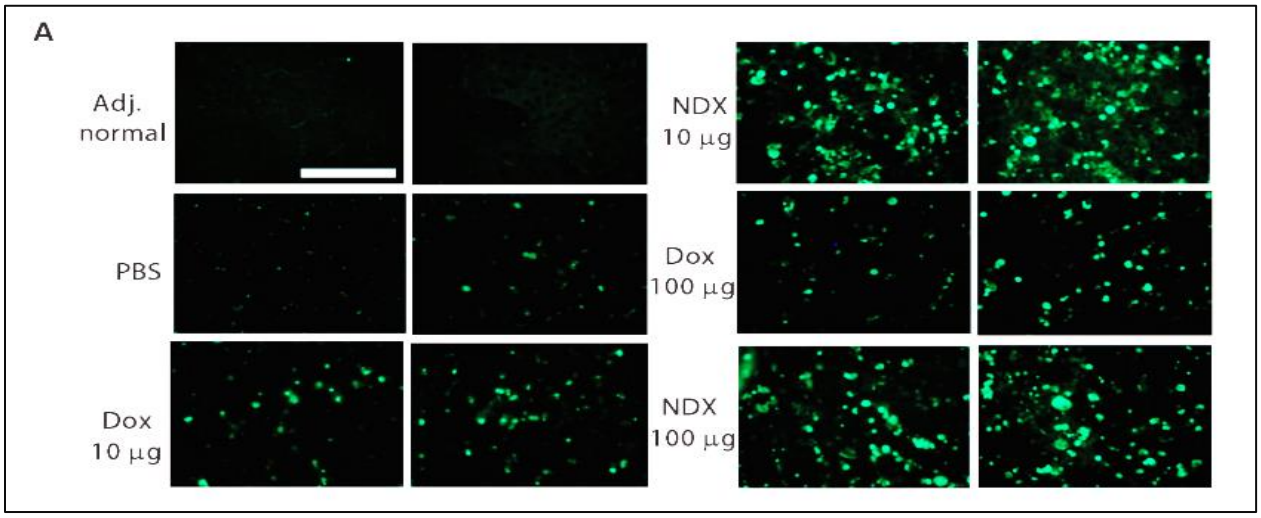

Figure 2.7.2.6 Increase in the drug tumor cell retention, allow for killing of tumor cells by sustain release of the NDX particles. (Delivery to murine liver cells).[121]

2.8 SIGNIFICANCE OF WORK, SPECIFIC AIMS, RESEARCH STRATEGY

2.8.1 RESEARCH STRATEGY

Pristine carboxylated nanodiamonds (pNDs) commonly assemble to form micron-sized aggregates. Therefore, the primary aim of this work was to develop an approach that could lead to a considerable disaggregation of NDs. The second aim is to functionalize the resulting disaggregated NDs using the biopolymer CS in the development of potential nanocarriers of chemotherapeutic agents.

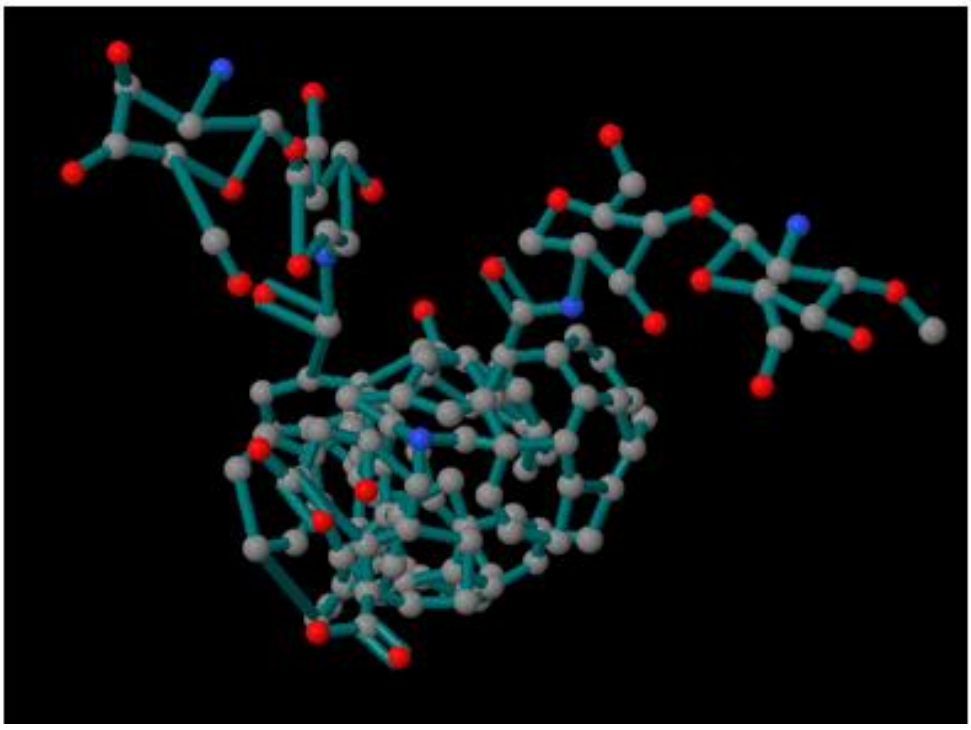

To serve the purposes of disaggregation and generation of positive charge on NDs, functionalization of NDs with chitosan, accompanied by mechanical disaggregation, will be studied. It is anticipated that the combined techniques will yield disaggregation of ND aggregate diamond particles, based upon the rationale that mechanical treatment by salt assisted milling

will disaggregate the agglomerates and the subsequent chitosan functionalization on the NDs surfaces will generate inter-particle steric hindrances, thereby circumventing their re-aggregation. As a result, zeta potential measurements should indicate a more positive and stable dispersion. Moreover, the presence of positive charges on the surfaces of the CS functionalized NDs would contribute largely to longer term dispersion stability generated by inter-particle repulsive behavior.

To verify the successful functionalization of ND-COOH with CS, X-ray Diffraction (XRD), Fourier Transform Infrared spectroscopy (FTIR). Thermogravimetric Analysis (TGA) was performed to quantitate the surface loading on the ND surfaces. To determine if the current approach of salt assisted milling was effective in inducing disaggregation of the ND aggregates, dynamic light scattering (DLS), zeta potential, Particle Size Analysis (PSA), and transmission electron microscopy (TEM) measurements were carried out. Dynamic light scattering measures the hydrodynamic diameter of the material, hence useful in determining the actual size of the particles; whereas transmission electron microscopy will assist in visualization of particles, hence suitable to provide a visual evidence of disaggregation. In addition, the zeta potential of the functionalized nanodiamonds (ND-COOH-CS) will be measured to assess surface charge and stability because the surface of the complex should possess positive charge for effective interaction with the cell surface to enable cellular uptake.

2.8.2 SIGNIFICANCE OF WORK

The significance of this work lies in the generation of next generation drug delivery systems (DDS) utilizing nanodiamond as the vehicle. Therefore, the aim of this work was to develop a methodology to generate a disaggregated population of NDs functionalized with the

biopolymer CS that could serve as vectors to deliver chemotherapeutic agents across the cellular membranes.

2.8.3 SPECIFIC AIMS

Mechanical salt assisted ball milling of detonation nanodiamonds will lead to their significant disaggregation.

The resulting nanodiamond particles will bind to the chitosan biopolymer via covalent boding forming nano-sized complexes

2.8.4 OBJECTIVES

The main objectives of this work are as follows:

(1) To investigate the use of salt assisted ball milling to minimize aggregation and decrease size distribution of the nanodiamond agglomerates.

(2) To synthesize and fully characterize the physicochemical properties of the ND-COOH system to confirm successful functionalization of the nanodiamond-chitosan composite (ND-COOH-CS)

To study the optical properties of nanodiamonds and assure the optical properties are maintained after functionalization.

CHAPTER 3

MATERIALS AND METHODS

3.1 Materials

Carboxylated Nanodiamonds (ND-COOH) (> 98% purity, cubic phase) with a particle size between 4-5 nm and 90 nm aggregate size were purchased from International Technology Center and used as the main concentration for the study of surface modification. Medium Molecular Weight Chitosan (β-1,4-linked N-acetyl-D-glucosamine (GlcNAc)) was purchased from Sigma Aldrich and used to modify the surfaces of the ND-COOH materials. Fluorescent ND >500 NV / particle, 90 nm average particle size diluted in a solution of 1 mg/mL of deionized water was used in comparison to ND-COOH. 500 mL Trifluoroacetic acid was purchased from Fisher Scientific. Using Cui et al. experiment, Amine NDs (N-NDs) (>98% purity, cubic phase) with a particle size of 4-5 nm and 60-80 nm aggregate size was used concerning the electrostatic attraction phenomenon. Sodium Chloride (NaCl) and Alginate were both purchased from Sigma Aldrich to reconstruct the experiment similarly to this experiment.

3.2 PREPARATION OF CHITOSAN ND COMPLEX (ND-COOH-CS)

0.1 M TFA solution was added into 100 mL of Millipore water and mixed thoroughly. 0.1 mg of CS was then added per mL of TFA/water solution, mixed and then stored into a beaker. The CS solution was then sonicated in the beaker for up to two hours and then stored in the refrigerator. 0.250 mg of ND-COOH was then added into a scintillation vial, and 4 mL of the CS solution was then added into the scintillation vial. The ND solution was then placed inside of the sonicator for two hours, and mixed thoroughly to make the ND-COOH-CS composites.

Furthermore, an Erlenmeyer flask was used to excrete the liquid byproduct. A stir bar was then placed in the suspended ND mixture, and the scintillation vial was placed on the hot plate at 100 °C for 10 hours until the remaining solution was evaporated and the product was formed.

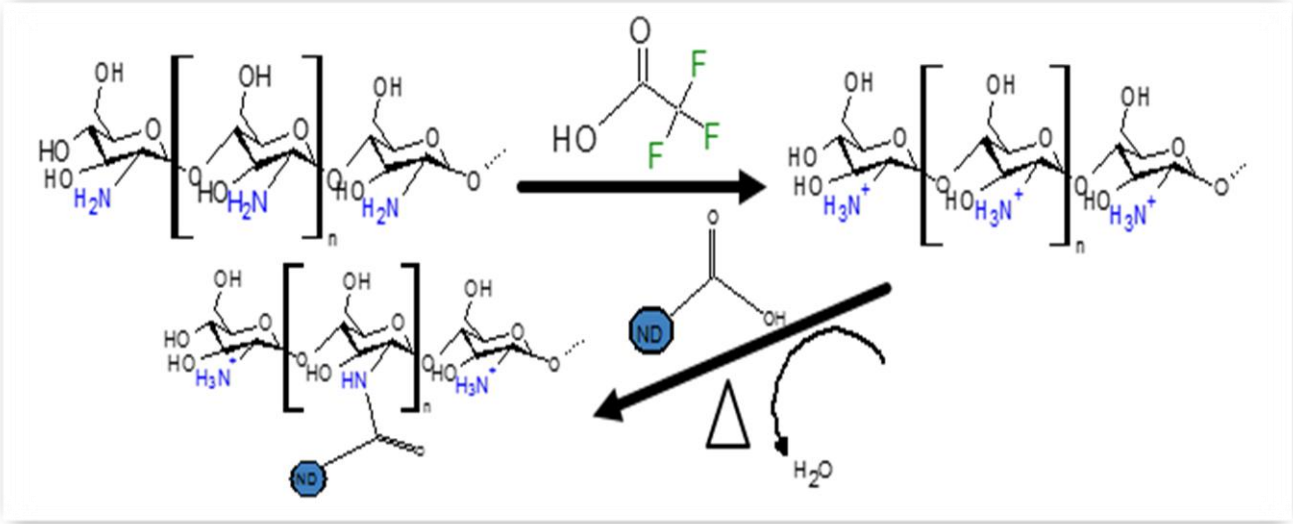

Figure 3.2 The Protonation of the CS Bioconjugate attached to the Surface of the ND-COOH.

3.3 Experimental

3.3.1 SALT-ASSISTED ATTRITION BALL MILLING

The attrition mill is Union Process Model HD01 and the steel balls are AISI 440-C (1/4"). Nanodiamond materials were measured at a 1:7 ratio with salt inside of a beaker. The salt (NaCl) grains were helpful in the de-agglomeration process of the nanodiamond particles as mentioned.[11-13] Titanium carbide ball milling beads were considered in this experiment and placed after the milling media was placed in the ball milling apparatus. Studies show, that the collision impact on the particles improves the efficacy of the ball milling method. The

optimization of ball milling took place as the machine was set for 2 h after setting up the series of experiments. After ball milling the ND-COOH with the media, the ND-COOH were then washed using Millipore water to separate the salt from the ND-COOH. ND-COOH pellets were then placed inside of centrifuge tubes, washed (x5) for five minutes each at 13,000 rpm. After the milling media solution was separated on the fifth ball milling attempt the supernatant was separated from the pellet and tested using $AgNO_3$ to see if any salt was left in the solution.

3.3.2 Dynamic Light Scattering (DLS)

DLS was measured using the Malvern Zetasizer Nano ZS. Nanodiamonds were filtrated and re-dispersed and sonicated in distilled water for up to 30 minutes. After nanodiamonds were sonicated, they were then diluted into a cuvette and placed into the DLS machine for the laser to penetrate through the clear side to gather accurate results for the intensity distributive curve of the Carboxylated nanodiamonds after ball milling took place.

3.3.3 ZETA POTENTIAL ANALYSIS (ZPA)

Zeta Potential analysis (ZPA) was measured using the Malvern Zetasizer Nano ZS. ZPA was used to confirm the stability within the surface chemistry of nanodiamond materials. The significance in zeta potential was to keep the particles suspended within the solution without causing them to crash into a stage of sedimentation known as phase separation. One of the major ways to keep the particles in a stable condition is by having charged particles that repel when dispersed into solutions. Uncharged particles have the tendency to get close enough to form aggregates. Disposable plastic cells were initially filled about three quarters and placed into the sample holder to tare the zeta potential analyzer. A dip cell was inserted into the disposable cell

so that the electrode was used to look at the motion of the particles due to the electric field. NDs were ball milled and sonicated for thirty mins and 1 mg was dispensed into a 1 mL cuvette. Once the solution was suspended a reading was taken to collect the data for the Carboxylated Nanodiamonds (ND-COOH) and the Carboxylated Nanodiamonds attached to the amide formation of the chitosan.

3.3.4 ATTENUATED TOTAL REFLECTION INFRARED SPECTROSCOPY (ATR-IR)

The Bruker Tensor 27 ATR-IR spectrometer was used to confirm the surface modification displayed on the ND-COOH structures using the chitosan. Prior to starting Using a spatula, a small sample was used to guide the probe containing the laser into the material used to identify surface functionality present within the ND-COOH, the ND-COOH-CS, and the CS material. The intensity was recorded in ATR spectra with wavenumber values ranging from 600-4000 nm^{-1}.

3.3.5 TRANSMISSION ELECTRON MICROSCOPY (TEM)

The TEM is a Zeiss Libra 120, and it was operated at 120kV. The camera used to acquire the images is a Gatan Ultrascan 1000 CCD. The Fluorescent Nanodiamonds were measured using the TEM instrument located in Cincinnati, Ohio in the National Risk Management Research Laboratory supported by the Environmental Protection Agency under the supervision of Dr. Sahle Demessie and Dr. Changseok Han. A TEM electron beam is produced, and it passes through the sample to imprint the image which is magnified by other lenses down to atomic sizes. The imprinted image is then recorded as an accurate measurement used to observe the materials on a nanoscale as the instrument can airlock and use its focusing mechanism for the

best results. TEM is used to give the identity of surface topology, and morphology of the materials.

3.3.6 X-RAY DIFFRACTION (XRD) ANALYSIS

The Bruker D8 XRD analyzer measured the crystallinity of materials in our experiments. XRD was used to measure the thermal degradation of the biopolymers and the pristine ND-COOH materials in comparison the modified ND-COOH-CS. Given that the NDs are abrasive materials we demonstrate the change in the degradation phase once the biopolymer is added to the surface of the pristine ND-COOH. Using this characterization technique, we can identify the point at which the temperature begins to degrade the samples to help us analyze how the modified ND-COOH-CS were modified.

3.3.7 THERMOGRAVIMETRIC ANALYSIS (TGA)

To determine the thermal degradation of the raw ND-COOH, raw CS, and modified ND-COOH, the TGA-DSC (Q600 Simultaneous TGA-DSC) was used to measure the point at which the temperature began degrading. Given that the NDs are abrasive materials, we demonstrate the change of the degradation phase is effected in the modified NDs as the thermal temperature decreases in comparison to the results of the raw ND-COOH.

CHAPTER 4

RESULTS AND DISCUSSION

4.1 DLS OF PRISTINE ND-COOH VS. SALT ASSISTED ATTRITION BALL MILLED ND-COOH

Nanodiamonds were filtrated and re-dispersed and sonicated in distilled water for up to 30 minutes. After nanodiamonds were sonicated, they were then diluted into a cuvette and placed into the DLS machine for the laser to penetrate through the clear side to gather accurate results for the intensity distributive curve of the Carboxylated nanodiamonds after ball milling took place. The results show ND-COOH reaching a 127.875 ± 1.1 nm from a 202-nm size giving evidence that the ball milling technique was indeed effective in terms of disaggregating the ND materials. The diameter size between the ND-COOH as supplied material in comparison to the 5 h ball milled ND-COOH have a 36.06% decrease again emphasizing the effective strategy for the salt attrition ball milling experiment. During this experiment, as the particle size decreases, no contamination is shown in the recorded data to further emphasize the elite ability and strategy oriented in the ball milling process.

The 5 h ball milling process demonstrates an effective decrease in diameter as viewed between the sizes of approximately (>555 nm). There is a decrease in intensity observed in comparison to the as supplied ND-COOH, supporting the theory that ball milling effectively decreases the size-ability of the ND particles. PDI of 5 h ball milled ND-COOH is ~ 0.241 nm ± 0.007 in comparison to the PDI confirming that there was also a decrease between the two molecular masses because of the salt assisted attrition ball milling process.

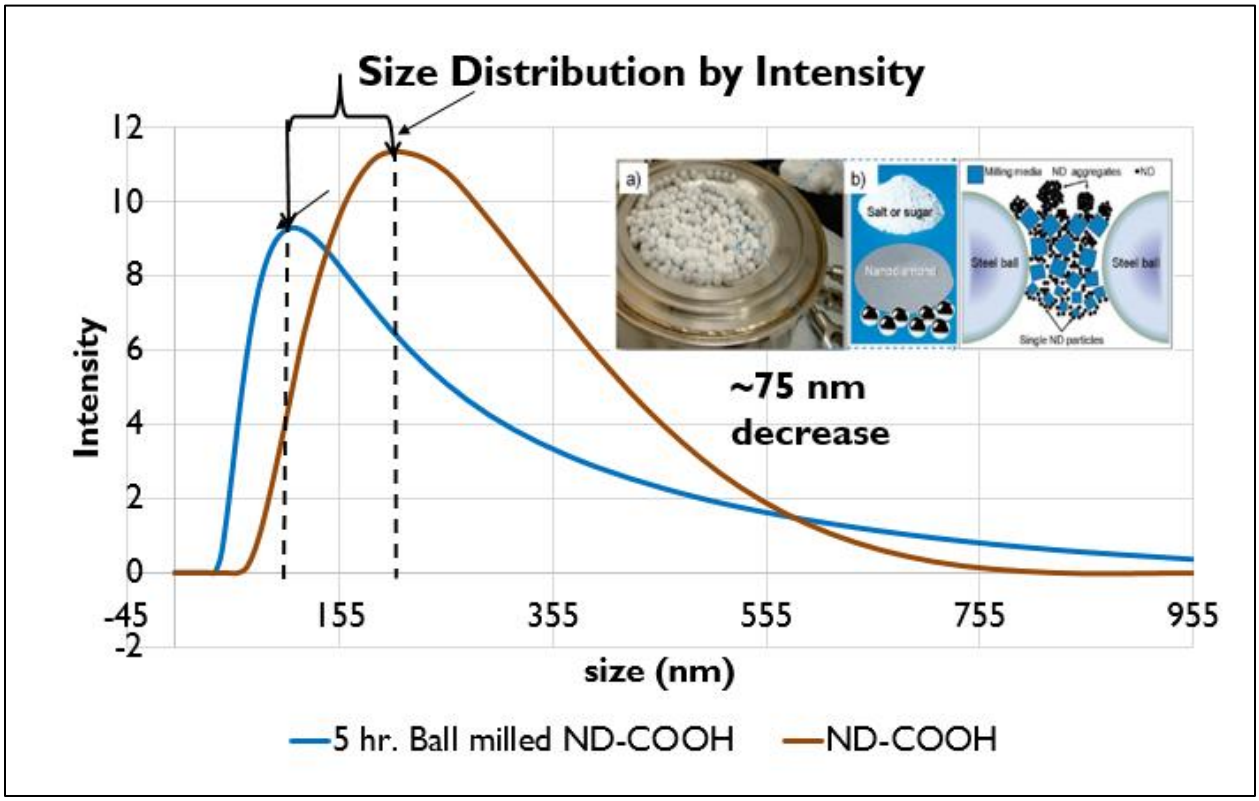

Figure 4.1 A comparison of as supplied ND-COOH vs. the 5-hr. ball milled ND-COOH DLS Size Distribution by Intensity plot.

4.1.1 DLS OF SURFACE MODIFIED PRISTINE NDs

To define the quantitative characteristics of the resulting suspensions DLS was used. In Figure 4.1.1, the analysis of the data allows the conclusion that most particles in the pristine ND suspension have an average diameter of size ~106 nm. However, upon increasing concentration of the CS concentration (0.25-1 w/v%), the particle size distribution increases due to an increasing hydrodynamic diameter of approximately 122.6 nm. At 1 w/v% concentration, the particle size distribution exceedingly approaches 1000nm. In consideration of zeta potential shown below, it can be observed that the stability advantageously increases with increase in

concentration. This was attributed to the ability of chitosan chains to compensate for the negative charges existing on the ND surface as well as ability to repel neighboring ND particles with the extension of chitosan chains on the surfaces of NDs. The CS being soluble in the TFA solution is a case for explaining the binding of the CS to the ND-COOH electrostatically and covalently.

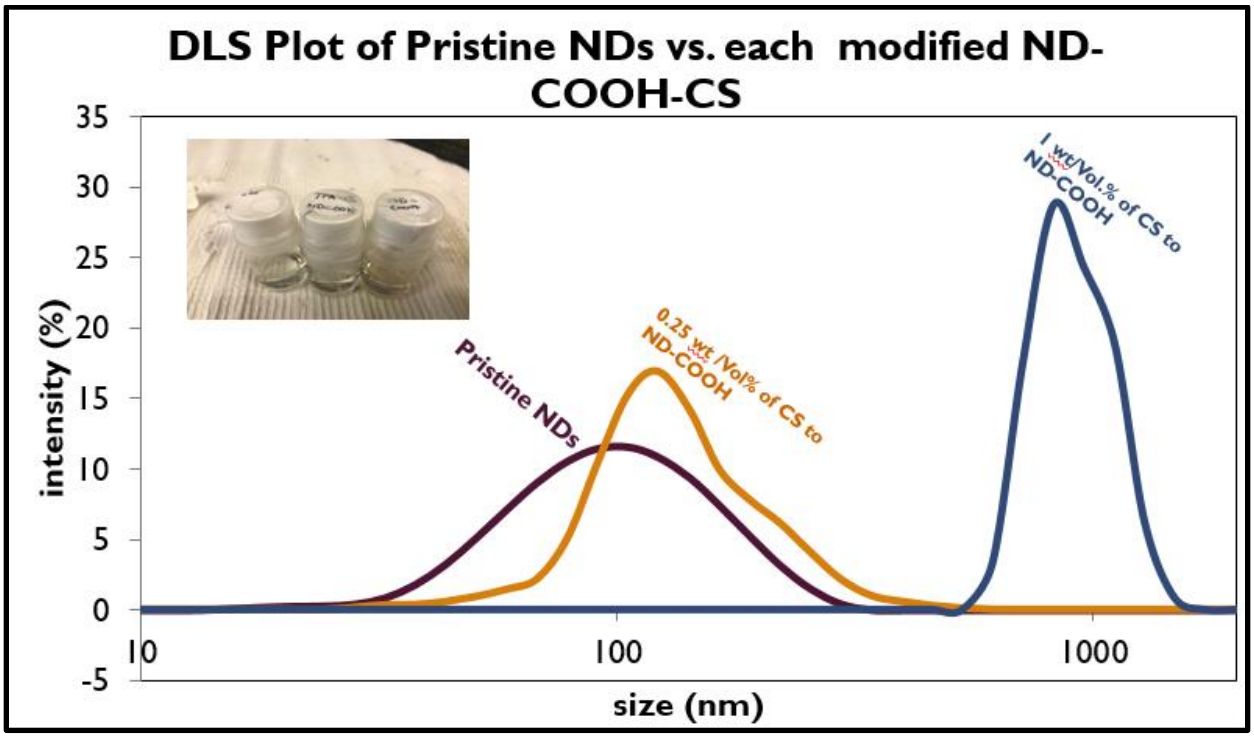

Figure 4.1.1 Size and zeta potential data were obtained on three different samples of each particle preparation (n = 3 per particle type). Size and zeta potential were measured in triplicate in each sample (triplicate analyses).

4.2 ZPA OF SURFACE MODIFIED PRISTINE NDS

The successful functionalization of NDs with CS was also confirmed by the zeta potential measurements. The pristine NDs showed a negative zeta potential of −40 mV, suggesting that negatively charged surface functional groups such as carboxylate were present. After functionalization with CS at 0.25w/v%, the mean zeta potential shifted to −26.7 mV, indicating

an increase in the density of positively charged surface groups. As expected, further functionalization at 1 w/v% of CS showed a positive zeta potential of +12.9 mV, demonstrating the predominance of a larger number of positively charged (amine) groups on their surfaces.

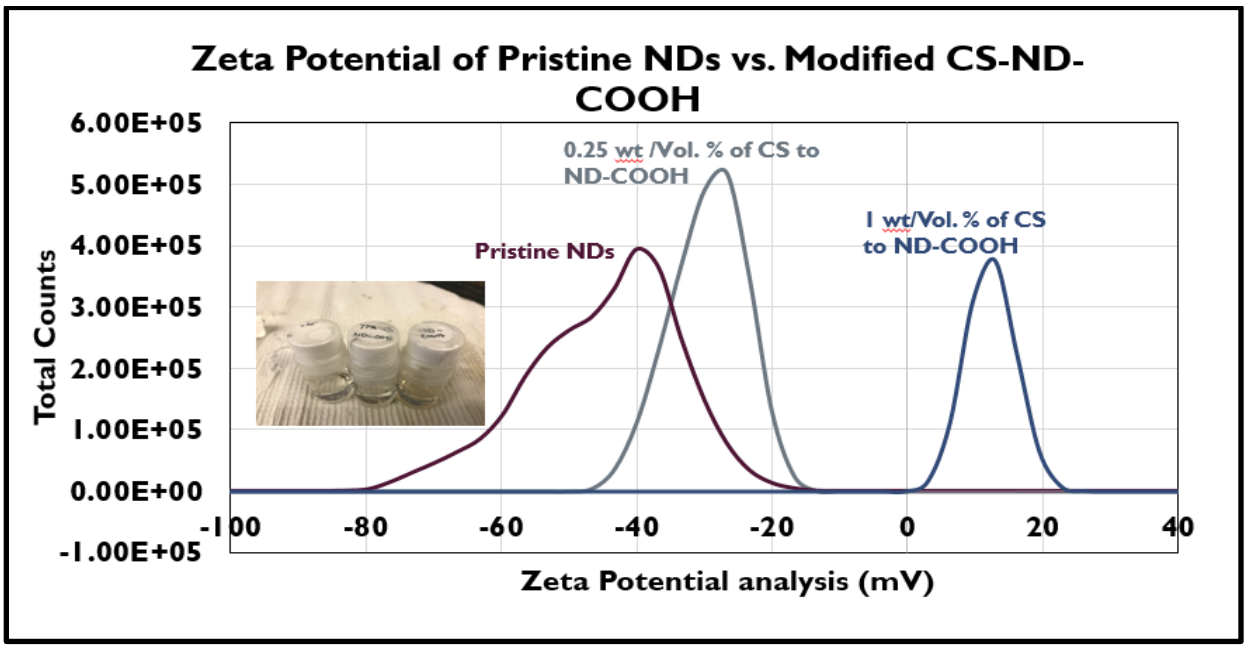

Figure 4.2 Zeta Potential data to illustrate the relationship of the Distributive Particle Size in Comparison to the Charge to emphasize electrostatic attraction between NDs and biopolymer.

4.3 XRD ANALYSIS OF SURFACE MODIFIED NDs vs. RAW MATERIALS

XRD proves the diamond structure of the particles. The observed peaks at 44, 75.5, and 91.5 represent signals from the diamond lattice. Upon modification of ND-COOH, we see the appearance of a diffuse band ~25 indicative of successful modification of the ND surface with CS. It is reported that nitrogen impurities (up to 2–3 wt.%), can form complexes in the core of nanodiamond particles, and the presence of twins and grain boundaries in the crystallites may

contribute to the broadening of the X-ray diffraction peaks that was earlier attributed to disordered sp^3 carbon as shown in the figure.

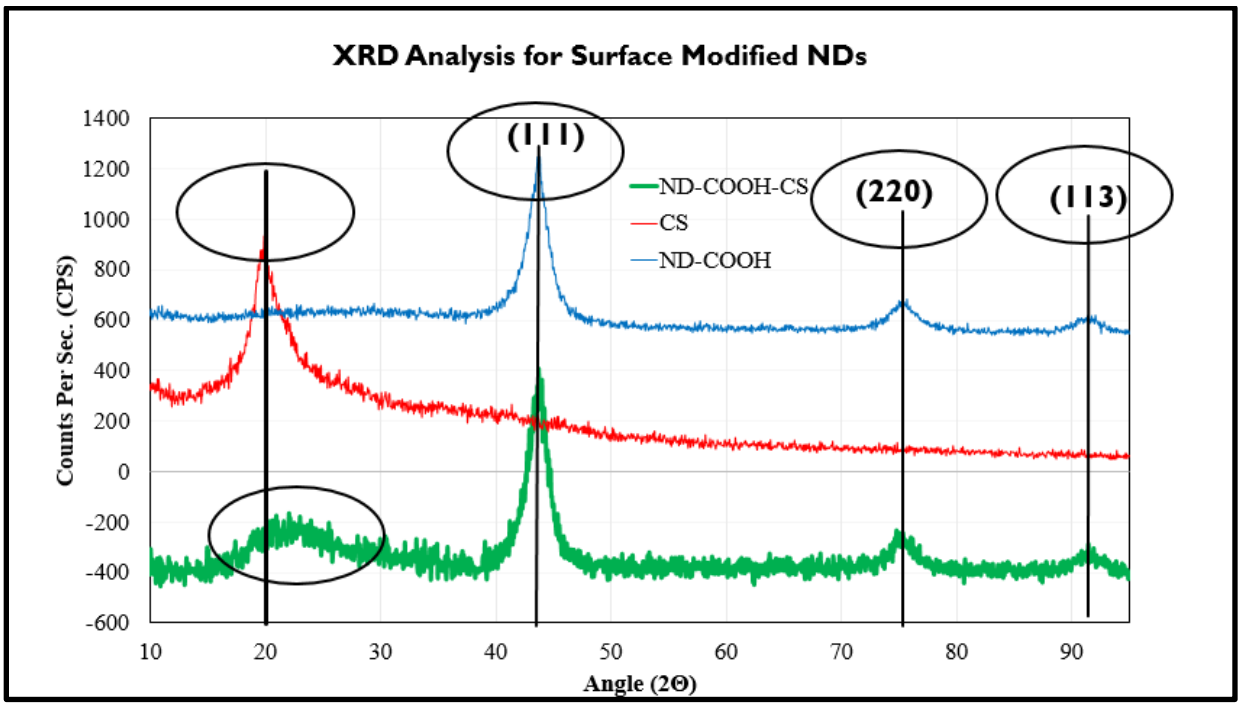

Figure 4.3 XRD Analysis used to illustrate the Surface Modification present on the NDs using the CS.

4.4 FTIR OF PRISTINE NDs IN COMPARISON TO RAW MATERIALS

FTIR of pristine ND showed characteristic bands at 1045 cm^{-1} and 1262 cm^{-1} due to vibrations of ether-like groups [43] are surmised to be generated from the covalent bonding of inter-carboxylic and/or hydroxyl groups, as well as bands in the C-H stretching region at 2900 cm^{-1} due to vibrations arising from the C-H bonds present on the surface of the NDs. It is reported that NDs exhibit a broad "fingerprint region" in literature ranging from 1000 to 1500 cm^{-1} [42]. It is important to note that the pristine ND were found to have features in the carbonyl

region (1760 cm^{-1}), suggesting that the raw material was already somewhat oxidized. The peaks at 1630 cm^{-1} (O-H bending) and 3400 cm^{-1} (O-H stretching) may have originated because of either the water adsorbed onto the NDs or the presence of covalently bonded hydroxyl functional groups on the surface of the NDs. Comparing the spectra of the ND-COOH-CS with those of pristine ND, it is evident from both the peak height and shape of the band located at 1630 cm^{-1} that the functionalization reaction was successful. The presence of an amide I band from 1640 to 1690 cm^{-1} and an amide II shoulder from 1510 to 1580 cm^{-1} in the ND-COOH- CS spectrum provide further evidence of functionalization.

Table 4.4 A Table Displaying the Spectral Features of ND-COOH & CS vs. Modified NDs.

Materials	Spectral Features cm^{-1}			
ND-COOH (B)	3100-3500 (-OH)	1650 (C=O)	1000 (-C-O)	~2887.57(C-H)
ND-COOH-CS (G)	3700-3500 R(C=O)NH	Amide (C=O) (1690-1630)	1700-1740 R(C=O)NH	1192.06 (R-NH)
CS (R)	3300-3500 (NH2) doublet	1375.31 (R-N-H)	2877.92 (Alkane)	1031.92 (1°-OH)

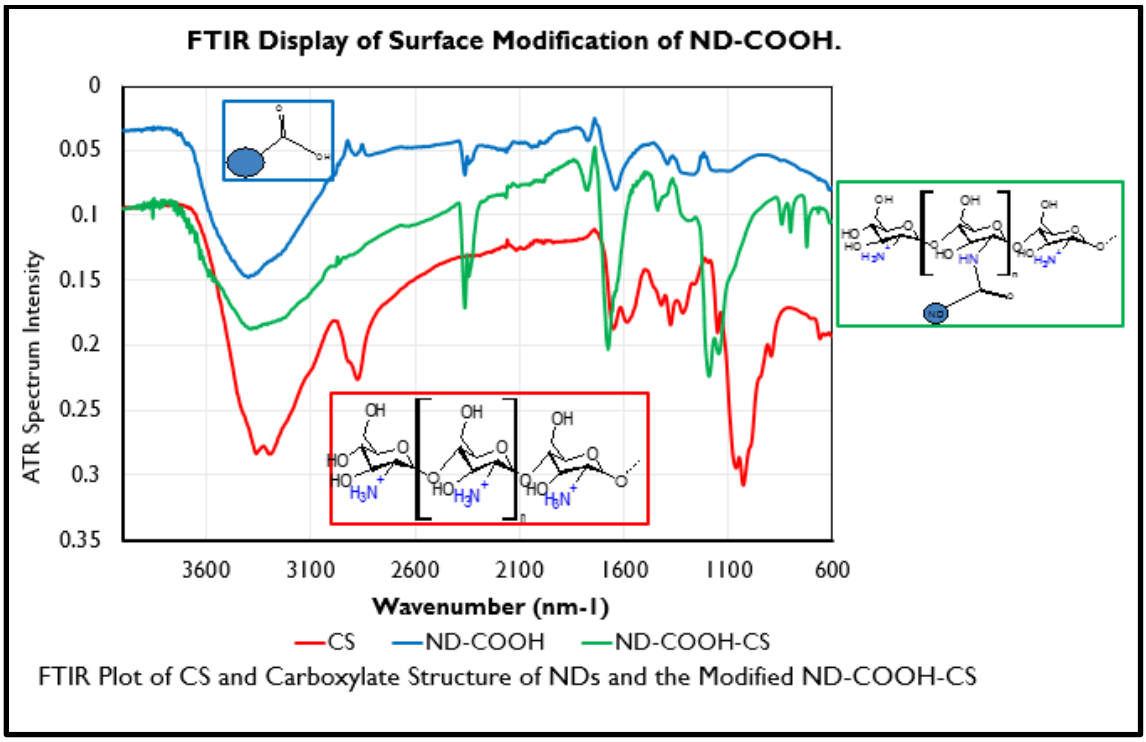

Figure 4.4 ATR-IR spectra of Carboxylated Nanodiamonds (ND-COOH), Chitosan (CS) Surface Modified ND-COOH (ND-COOH-CS).

4.5 TGA OF PRISTINE AND CS MODIFIED ND-COOH

Thermogravimetric analyses were performed to provide quantitative estimates of the surface loading of functional groups attached to the NDs. The thermograms of the pristine NDs and ND-COOH-CS showed initial weight loss at 100 $^{\circ}$C due to loss of water. The thermogram of the ND-COOH-CS showed no appreciable weight loss from 100-250C indicating thermal stability of the functionalized NDs. The surface loading of the ND-COOH-CS was calculated from the thermogram. If the surfaces of NDs are dominated by carboxylate groups, the estimated surface coverage was. The high surface functionalization confers high CS binding capacity to the nanomaterial.

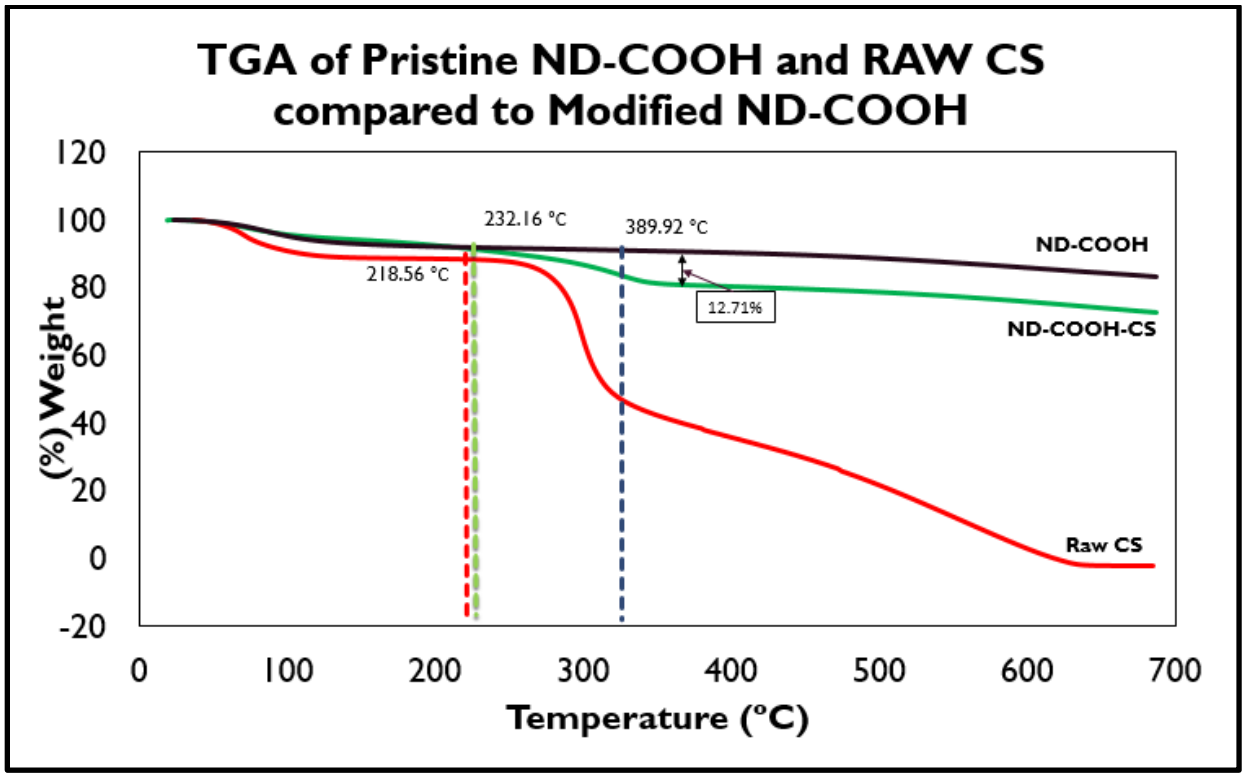

Figure 4.5 TGA of ND-COOH and Raw CS compared to the modified ND-COOH-CS used to demonstrate the surface modification of the pristine ND-COOH.

4.6 CROSS CORRELATION SPECTROPHOTOMETRY (CCS)

Figure 4.6.1 shows emission spectra (λmax = 578 nm) of FNDs and ND-COOH. The FND spectrum, acquired for particles suspended in water and excited with a continuous-wave (cw) 488-nm laser, reveals the N-V centres existing inside the material: $(N\text{-}V)^-$ with a phonon line at 576.1nm and 637nm. Likewise, the emission spectra of ND-COOH (Figure 4.6.2) shows the N-V centres inside the material at ~576nm. Comparing it with the spectrum of the control FND, indicates that the fluorescence spectra of the ND-COOH are essentially the same. The fluorescence intensities of these NDs are bulk-dependent, little affected by their surface characteristics and, therefore, their environments. Notably, the excellent photostability (that is,

no photobleaching or photoblinking) of the material is preserved. This application may demonstrate that there is an optical application that may be considered in the future for examining these ND particles for in vitro studies.

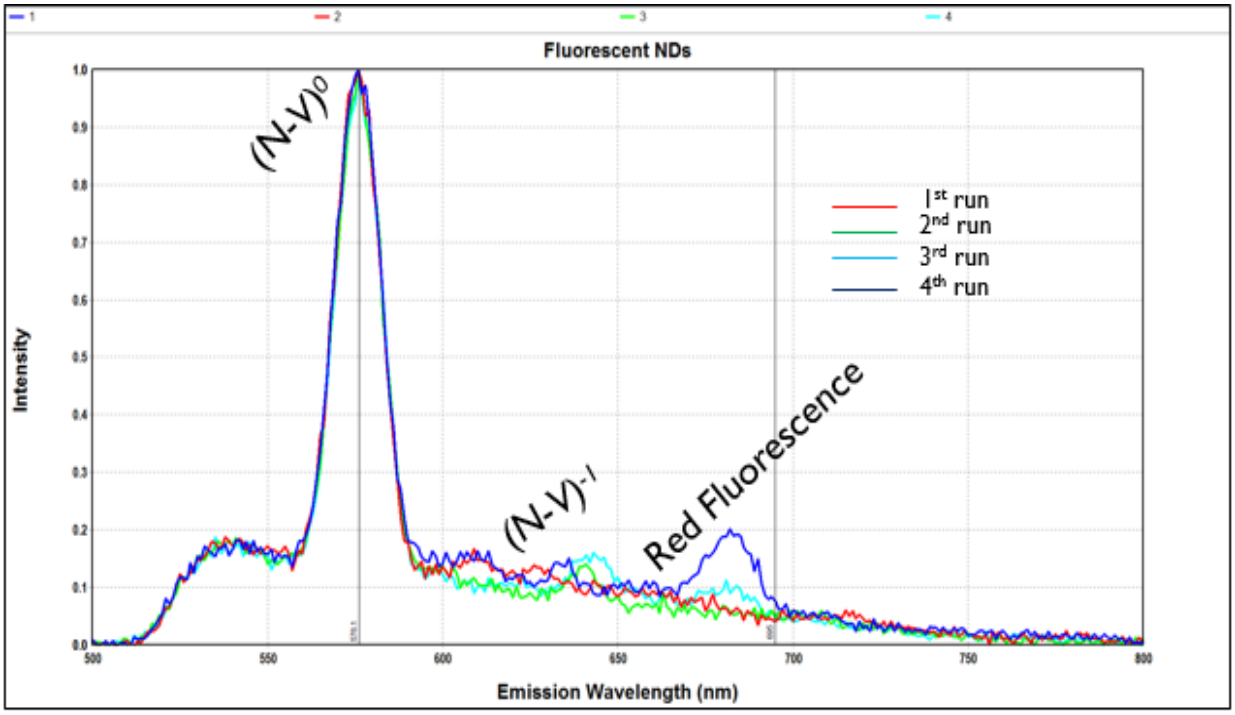

Figure 4.6.1 The Cross-Correlation Emission Spectrum of the Red Fluorescent NDs (commercially purchased) demonstrating the emission spectra given a 488-nm lens at the wavelength 576.1-nm and ~695-nm.

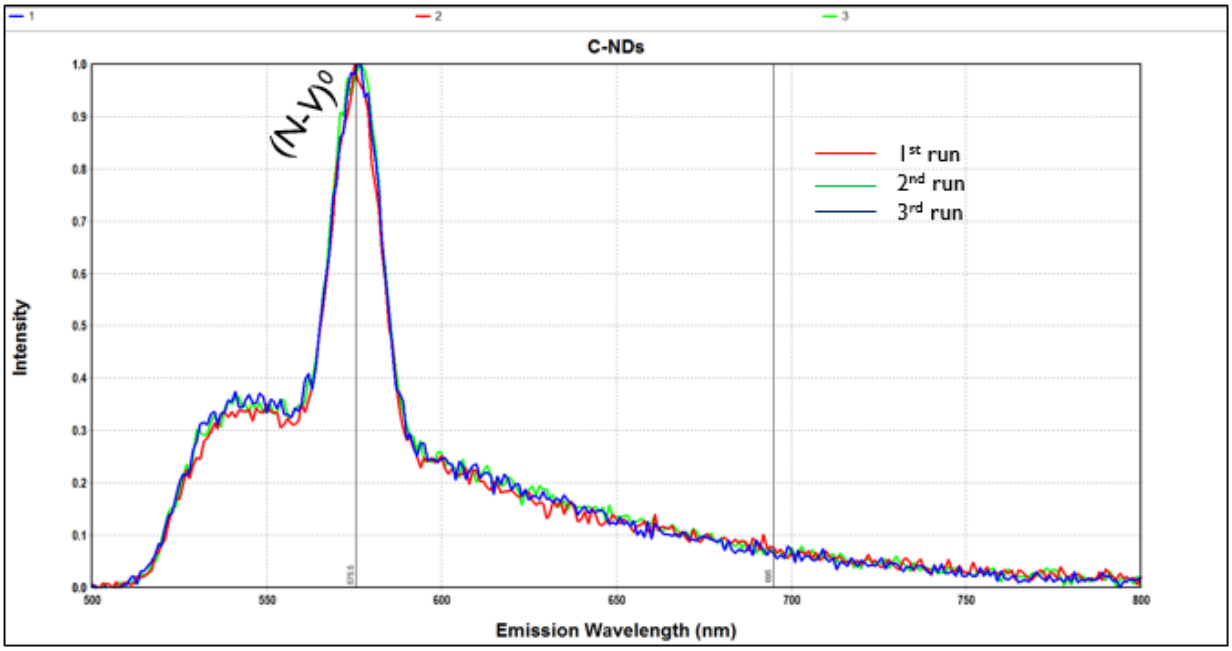

Figure 4.6.2 The Cross-Correlation Emission Spectrum of the ND-COOH demonstrating the emission spectra using a 488-nm lens giving the wavelength 576.1 nm.

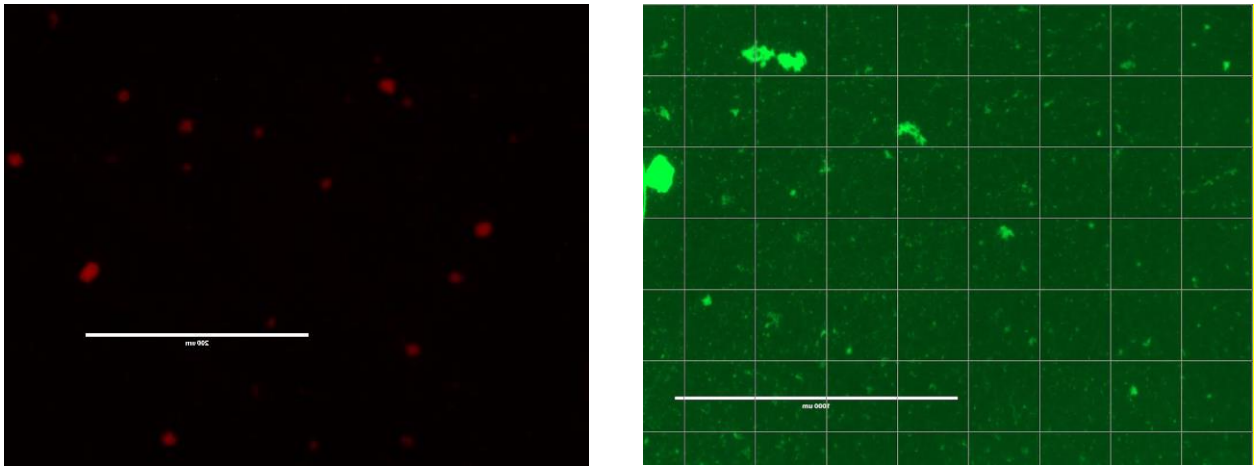

Figure 4.6.3 Evos Microscopic Imaging of Sigma Aldrich Red Fluorescent NDs (Left) compared to as supplied ND-COOH (Right). Evos Microscopy demonstrates the Red Fluorescent the uniformity of the Red fluorescent NDs in comparison to ND-COOH which have more aggregation.

4.7 TRANSMISSION ELECTRON MICROSCOPY (TEM) OF Red fNDs vs. ND-COOH and ND-COOH-CS

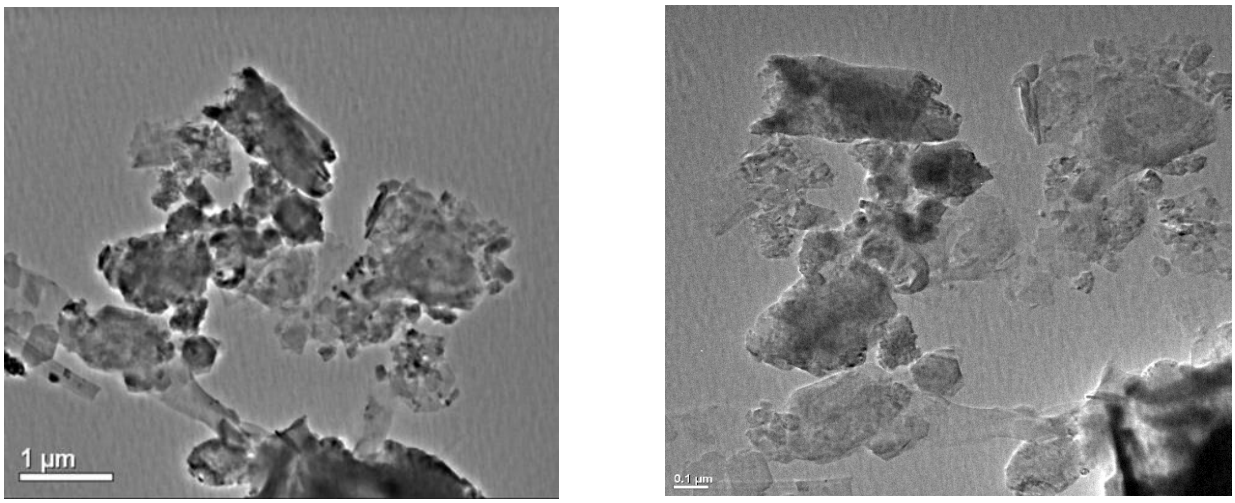

Figure 4.7.1 TEM images of the Red Fluorescent Nanodiamonds. a. Fluorescent ND. Measure at 1000 nm b. Fluorescent NDs measured at 100 nm.

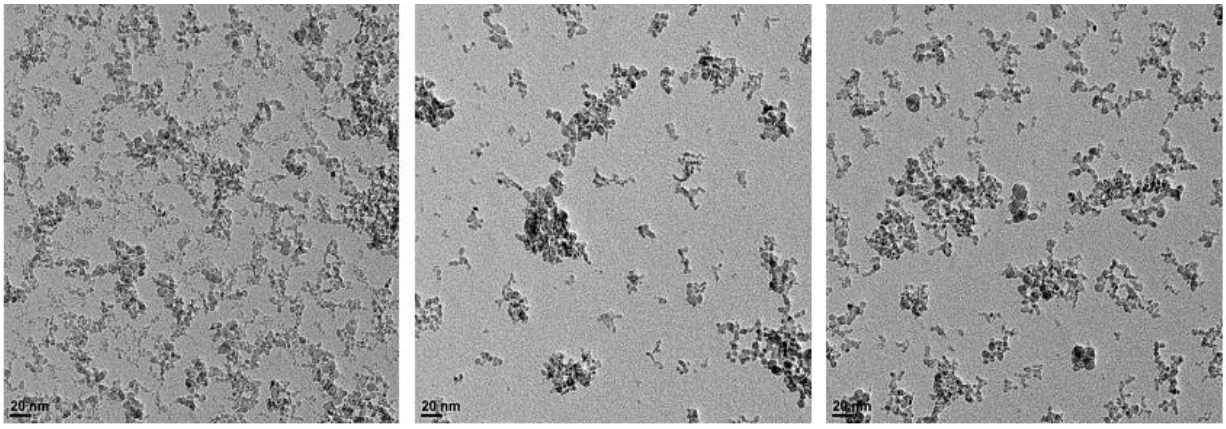

Figure 4.7.2 TEM images of the pristine ND-COOH (*left*), 0.25 wt./vol% ND-COOH-CS (*center*), 1 wt./vol% of ND-COOH-CS (*right*). (All measured on a 20-nm scale)

Observations by transmission electron microscopy show that pristine nanodiamond particles are overcome by aggregation, which show particles with lateral dimensions ranging up to several hundred nanometers but with flattened, plate-like structures, which appear to aggregate in stacks. The lateral dimensions of the individual particles are somewhat larger than the mass-weighted size determined by DLS; however, this presumably reflects the very nonspherical particle shapes. This aggregation may be due to partial coatings of graphitic shell or amorphous carbon with dangling bonds terminated by functional groups. TEM imaging showed that NDs have a polygonal shape. In addition to the ND size indicated by dynamic light scattering analysis, very small mfNDs (a few nm) were detected within the ND aggregates by TEM. The 1 μm scale bar images focus on one of the large particles, which is shown to be an aggregate of many NDs.

TEM images of the 0.25 w/v% CS-ND-COOH show more dispersed and smaller size aggregates with more evidence of individual single particle ND. Thereby, providing further evidence that modification of NDs with the biopolymer chitosan facilitates dispersion and stability of NDs as observed in zeta potential analysis.

CHAPTER 5

CONCLUSION

5.1 CONCLUSION

In this work, ND-COOH were functionalized with the biopolymer, CS. Favorable interactions developed between the surface of NDs and chitosan polymer chains were attributed to the presence of numerous carboxyl groups on the ND surfaces facilitating covalent bonding between the COOH and NH_2 on chitosan. The chains synthesized at the surface of ND-COOH-CS were observed to be adsorbed strongly at the surface of NDs with the formation of amide bonds between carboxyl groups and NH_2. Stability of functionalized ND dispersions as determined though zeta potential analysis is attributed to the extension of these polymer chains creating repulsion from neighboring ND particles. Although electrostatic interactions due to opposite zeta potential values between NDs and chitosan cannot be completely excluded, the contribution of this repulsion between functionalized NDs to the stability of the complex can also serve as facilitating the charge screening effect. TEM displays modified NDs not interacting with pristine NDs due to the repulsive effect because of the ND-COOH hypothetically binding to the backbone structure of the Chitosan's NH_2 group. FTIR and TGA confirms the surface modification of the ND-COOH structure as there are more intense bands displayed in the FTIR spectra, and there is more thermal degradation seen in TGA because of the biopolymer binding to the NDs. NDs were successfully functionalized with chitosan producing surface loading of mmol g^{-1} of ND. These modified NDs formed highly stable aqueous dispersions with an optimal zeta potential of ~+12.9mV at 1 w/v%.

5.2 FUTURE WORK

Based on promising results, further work is recommended in the following areas:

(1) Investigating the loading capacity of NDs for optimal biocompatibility.

(2) Exploring the drug loading and the release studies (possibly doxorubicin (DOX) or cisplatin (DDP).

(3) Exploring the ex vivo analysis of ND interaction with MCF-7 cells

(4) Finding the optical properties and intracellular transport of the ND-COOH-CS using CLSM and cross correlation photospectrometry.

REFERENCES

1. Osawa E. Single-nano buckydiamond particles: synthesis strategies, characterization methodologies and emerging applications. In: Ho D, editor. Nanodiamonds-applications in biology and nanoscale medicine; New York: Springer Science+Business Media; 2010:1-33.

2. Baidakova M, Vul' A. New prospects and frontiers of nanodiamond clusters. J Phys D: Appl Phys. 2007;40:6300–6311.

3. Chang IP, Hwang KC, Chiang CS. Preparation of fluorescent magnetic nanodiamonds and cellular imaging. J Am Chem Soc. 2008;130:15476–15481.

4. Chang YR, Lee HY, Chen K. et al. Mass production and dynamic imaging of fluorescent nanodiamonds. Nat Nanotechnol. 2008;3:284–288.

5. Chao JI, Perevedentseva E, Chung PH. et al. Nanometer-sized diamond particle as a probe for biolabeling. Biophys J. 2007;93:2199–2208.

6. Pramatarova L, Dimitrova R, Spassov EPT. et al. Peculiarities of hydroxyapatite/nanodiamond composites as novel implants. J Phys Conf Ser. 2007;93:012049.

7. Huang H, Pierstorff E, Osawa E. et al. Active nanodiamond hydrogels for chemotherapeutic Delivery. Nano Lett. 2007;7:3305– 3314.

8. Xing Y, Dai L. Nanodiamonds for Nanomedicine. Nanomedicine. 2009;4:207–218.

9. Li J, Zhu Y, Li WX. et al. Nanodiamonds as intracellular transporters of chemotherapeutic drug. Biomaterials. 2010;31:8410–8418.

10. Schrand AM, Huang HJ, Carlson C. et al. Are diamond nanoparticles cytotoxic? J Phys Chem B. 2007;111:2–7.

11. Schrand A, Dai L, Schlager J. et al. Differential biocompatibility of carbon nanotubes and nanodiamonds. Diam Relat Mater. 2007;16:2118–2123.

12. Liu K, Cheng C, Chang C. et al. Biocompatible and detectable carboxylated nanodiamond on human cell. Nanotechnology. 2007;18:325102.

13. Liu K K, Wang C C, Cheng C L. et al. Endocytic carboxylated nanodiamond for the labeling and tracking of cell division and differentiation in cancer and stem cells. Biomaterials. 2009;30:4249–4259.

14. Xing Y, Xiong W, Zhu L. et al. DNA damage in embryonic stem cells caused by nanodiamonds. ACS Nano. 2011;5:2376–2384.

15. Magrez A, Kasas S, Salicio V. et al. Cellular toxicity of carbon-based nanomaterials. Nano Lett. 2006;6:1121–1125.

16. Zhang XY. Biological effects of three kinds of carbon nanomaterials; Dissertation for the Doctoral Degree. Shanghai: Shanghai Institute of Applied Physics, CAS; 2010. pp. 61–64.

17. Vaijayanthimala V, Tzeng YK, Chang HC. et al. The biocompatibility of fluorescent nanodiamonds and their mechanism of cellular uptake. Nanotechnology. 2009;20:425103.

18. Yuan Y, Wang X, Jia G. et al. Pulmonary toxicity and translocation of nanodiamond in mice. Diam Relat Mater. 2010;19:291–299.

19. Zhang XY, Yin JL, Kang Cheng. et al. Biodistribution and toxicity of nanodiamonds in mice

after intratracheal instillation. Toxicol Lett. 2010;198:237–243.

20. Lam CW, James JT, McCluskey R. et al. Pulmonary toxicity of single-wall carbon nanotubes in mice 7 and 90 days after intratracheal instillation. Toxicol Sci. 2004;77:126–134.

21. Warheit BD, Laurence BR, Reed KL. et al. Comparative pulmonary toxicity assessment of single wall carbon nanotubes in rats. Toxicol Sci. 2004;77:117–125.

22. Muller L, Huaux F, Moreau N. et al. Respiratory toxicity of multi-wall carbon nanotubes. Toxicol Appl Pharmacol. 2005;207:221–231.

23. Schrand AM, Hens SAC, Shenderova OA. Nanodiamond particles: properties and perspectives for bioapplications. Crit Rev Solid State. 2009;34:18–74.

24. Puzyr AP, Baron AV, Purtov KV. et al. Nanodiamonds with novel properties: a biological study. Diamond Relat Mater. 2007;16:2124–2128.

25. Bakowicz K, Mitura S. Biocompatibility of NCD. Journal of Wide Bandgap Materials. 2002;9:261–272.

26. Li QN, Xiu Y, Zhang XD. et al. Preparation of ^{99m}Tc-C_{60}(OH)x and its biodistribution studies. Nucl Med Biol. 2002;29:707–710.

27. Li YG, Zhang XD, Li QN. et al. Radioodination of C_{60} derivative $C_{60}(OH)_x(O)_y$. J Radioanal Nucl Ch. 2001;250:363–364.

28. Wang HF, Wang J, Deng XY. et al. Biodistribution of carbon single-walled nanotubes in mice. J Nanosci Nanotechnol. 2004;4:1019–1024.

29. Singh R, Pantarotto D, Lacerda L. et al. Tissue biodistribution and blood clearance rates of intravenously administered carbon nanotube radiotracers. PNAS. 2006;28:3357–3362.

30. Liu Z, Cai WB, He L. et al. In vivo biodistribution and highly efficient tumor targeting of carbon nanotubes in mice. Nat Nanotechnol. 2007;2:47–50.

31. Guo JX, Zhang X, Li QN. Biodistribution of functionalized multi-wall carbon nanotubes in mice. Nucl Med Biol. 2007;34:579–583.

32. Yuan Y, Chen YW, Liu JH. et al. Biodistribution and fate of nanodiamonds in vivo. Diamond Relat Mater. 2009;18:95–100.

33. Rojas S, Gispert JD, Martin R. et al. Biodistribution of amino-functionalized diamond nanoparticles. In vivo studies based on ^{18}F radionuclide emission. ACS Nano. 2011;5:5552–5559.

34. Jia NQ, Lian Q, Shen HB. et al. Intracellular delivery of quantum dots tagged antisense oligodeoxynucleotides by functionalized multiwalled carbon nanotubes. Nano Lett. 2007;7:2976–2980.

35. Liu Z, Sun XM, Nakayama-Ratchford N. et al. Supramolecular chemistry on water-soluble carbon nanotubes for Drug Loading and Delivery. ACS Nano. 2007;1:50–56.

36. Zhang LM, Lu ZX, Zhao QH. et al. Enhanced chemotherapy efficacy by sequential delivery of siRNA and anticancer drugs using PEI-grafted graphene oxide. Small. 2011;7:460–464.

37. Huang P, Xu C, Lin J. et al. Folic acid-conjugated graphene oxide loaded with photosensitizers for targeting photodynamic therapy. Theranostics. 2011;1:240–250.

38. Zhang XK, Meng LJ, Lu QH. et al. Targeted delivery and controlled release of doxorubicin to cancer cells using modified single wall carbon nanotubes. Biomaterials. 2009;30:6041–6047.

39. Manna SK, Sarkar S, Barr J. et al. Single-walled carbon-nanotube induces oxidative stress and activates nuclear transcription factor-κB in human keratinocytes. Nano Lett. 2005;5:1676–1684.

40. Zhang YB, Ali SF, Dervishi E. et al. Cytotoxicity effects of graphene and single-wall carbon nanotubes in neural phaeochromocytoma-derived PC12 cells. ACS Nano. 2010;4:3181–3186.

41. Wang JY, Sun PP, Bao YM. et al. Cytotoxicity of single-walled carrbn nanotubes on PC12 cells. Toxicol in vitro. 2011;25:242–250.

42. Hartl A, Schmich E, Garrido JA. et al. Protein-modified nanocrystalline diamond thin films for biosensor applications. Nat Mater. 2004;3:736–742.

43. Liu Y, Khabashesku VN, Halas NJ. Fluorinated nanodiamond as a wet chemistry precursor for diamond coatings covalently bonded to glass surface. J Am Chem Soc. 2005;127:3712–3713.

44. Huang HJ, Pierstorff E, Osawa E. et al. Protein-mediated assembly of nanodiamond hydrogels into a biocompatible and biofunctional multilayer nanofilm. ACS Nano. 2008;2:203–212.

45. Huang HJ, Dai LM, Wang DH. et al. Large-scale self-assembly of dispersed nanodiamonds. J Mater Chem. 2008;18:1347–1352.

46. Lam R, Chen M, Pierstorff E. et al. Nanodiamond-embedded microfilm devices for localized chemotherapeutic elution. ACS Nano. 2008;2:2095–2102.

47. Chow EK, Zhang XQ, Chen M. et al. Nanodiamond therapeutic delivery agents mediate enhanced chemoresistant tumor treatment. Sci Transl Med. 2011;3:73ra21.

48. Adnan A, Lam R, Chen HN. et al. Atomistic simulation and measurement of pH dependent cancer therapeutic interactions with nanodiamond carrier. Mol Pharmaceutics. 2011;8:368–374.

49. Chen M, Pierstorff ED, Lam R. et al. Nanodiamond-mediated delivery of water-insoluble therapeutics. ACS Nano. 2009;3:2016–2022.

50. Shimkunas RA, Robinson E, Lam R. et al. Nanodiamond-insulin complexes as pH-dependent protein delivery vehicles. Biomaterials. 2009;30:5720–5728.

51. Ma XW, Zhao YL, Liang XJ. Nanodiamond delivery circumvents tumor resistance to doxorubicin. Acta Pharmacol Sin. 2011;32:543–544.

52. Guan B, Zou F, Zhi JF. Nanodiamond as the pH-responsive vehicle for an anticancer drug. Small. 2010;6:1514–1519.

53. Li XX, Shao JQ, Qin Y. et al. TAT-conjugated nanodiamond for the enhanced delivery of doxorubicin. J Mater Chem. 2011;21:7966–7973.

54. Liu KK, Zheng WW, Wang CC. et al. Covalent linkage of nanodiamond-paclitaxel for drug delivery and cancer therapy. Nanotechnology. 2010;21:315106.

55. Wanga HD, Yang QQ, Niu CH. Functionalization of nanodiamond particles with N,O-carboxymethyl chitosan. Diam Relat Mater. 2010;19:441–444.

56. Purtov KV, Petunin AI, Burov AE. et al. Nanodiamonds as carriers for address delivery of biologically active substances. Nanoscale Res Lett. 2010;5:631–636.

57. Vaijayanthimala V, Chang HC. Functionalized fluorescent nanodiamonds for biomedical applications. Nanomedicine. 2009;4:47–55.

58. Yu SJ, Kang MW, Chang HC. et al. Bright fluorescent nanodiamonds: no photobleaching and low cytotoxicity. J Am Chem Soc. 2005;127:17604–17605.

59. Fu CC, Lee HY, Chen K. et al. Characterization and application of single fluorescent nanodiamonds as cellular biomarkers. Proc Natl Acad Sci. 2007;104:727–732.

60. Hurt RH, Monthioux M, Kane A. Toxicology of carbon nanomaterials: status, trends, and perspectives on the special issue. Carbon. 2006;44:1028–1033.

61. Zhu Y, Ran TC, Li YG. et al. Dependence of the cytotoxicity of multi-walled carbon nanotubes on the culture medium. Nanotechnology. 2006;17:4668–4674.

62. Casey A, Davoren M, Herzog E. et al. Probing the interaction of single walled carbon nanotubes within cell culture medium as a precursor to toxicity testing. Carbon. 2007;45:34– 40.

63. Casey A, Herzog E, Davoren M. et al. Spectroscopic analysis confirms the interactions between single walled carbon nanotubes and various dyes commonly used to assess cytotoxicity. Carbon. 2007;45:1425–1432.

64. Zhu Y, Li WX, Li QN. et al. Effects of serum proteins on intracellular uptake and cytotoxicity of carbon nanoparticles. Carbon. 2009;47:1351–1358.

65. Hu W B, Peng C, Lv M. et al. Protein corona-mediated mitigation of cytotoxicity of grapheme oxide. ACS Nano. 2011;5:3693–3700.

66. Faklaris O, Joshi V, Irinopoulou T, Tauc P, Sennour M, Girard H, Gesset Cl, Arnault J-

C,Thorel A, Boudou J-P, et al.: Photoluminescent Diamond Nanoparticles for Cell Labeling: Study of the Uptake Mechanism in Mammalian Cells. ACS Nano 2009, 3:3955-3962.

67. Liu KK, Wang CC, Cheng CL, Chao JI: Endocytic carboxylated nanodiamond for the labeling and tracking of cell division and differentiation in cancer and stem cells. Biomaterials 2009, 30:4249-4259.

68. Schrand AM, Dai L, Schlager JJ, Hussain SM, Osawa E: Differential biocompatibility of carbon nanotubes and nanodiamonds. Diamond and Related Materials 2007, 16:2118-2123.

69. Li J, Zhu Y, Li W, Zhang X, Peng Y, Huang Q: Nanodiamonds as intracellular transporters of chemotherapeutic drug. Biomaterials 2010, 31:8410-8418.

70. Schrand AM, Huang H, Carlson C, Schlager JJ, Osawa E, Hussain SM, Dai L: Are diamond nanoparticles cytotoxic? Journal of Physical Chemistry B 2007, 111:2-7.

71. Yu SJ, Kang MW, Chang HC, Chen KM, Yu YC: Bright fluorescent nanodiamonds: No photobleaching and low cytotoxicity. Journal of the American Chemical Society 2005,127:17604-17605.

72. Liu KK, Cheng CL, Chang CC, Chao JI: Biocompatible and detectable carboxylated nanodiamond on human cell. Nanotechnology 2007, 18:325102.

73. Chao JI, Perevedentseva E, Chung PH, Liu KK, Cheng CY, Chang CC, Cheng CL: Nanometer-sized diamond particle as a probe for biolabeling. Biophysical Journal 2007, 93:2199-2208.

74. Huang H, Pierstorff E, Osawa E, Ho D: Active nanodiamond hydrogels for chemotherapeutic

delivery. Nano Letters 2007, 7:3305-3314.

75. Schrand AM, Johnson J, Dai L, Hussain SM, Schlager JJ, Zhu L, Hong Y, Osawa E:Cytotoxicity and Genotoxicity of Carbon Nanomaterials. Safety of Nanoparticles: From Manufacturing to Medical Applications 2009:159-187.

76. Krafft C, Knetschke T, Siegner A, Funk RHW, Salzer R: Mapping of single cells by near infrared Raman microspectroscopy. Vibrational Spectroscopy 2003, 32:75-83.

77. Chung PH, Perevedentseva E, Cheng CL: The particle size-dependent photoluminescence of nanodiamonds. Surface Science 2007, 601:3866-3870.

78. Colpin Y, Swan A, Zvyagin AV, Plakhotnik T: Imaging and sizing of diamond nanoparticles.Optics Letters 2006, 31:625-627

79. Mochalin, V., Gogotsi, Y., Nanodiamond–Polymer Composites. Diamond Relat. Mater. 58 (2012) 161–171

80. Cui, Z., Zhang, Y., Zhang, Kong H., Tang, X., Pan, L., Xia, K., Aldalbahi, Li d, A., Tai R., Fan C., Zhu, Y. Sodium alginate-functionalized nanodiamonds as sustained chemotherapeutic drug-release vectors CARBON 97 (2016) 78–86

81. Burleson, T., Yusuf, N., Stanishvesky, A. JAMME Vol. 37 (2009) 258-263

82. Mochalin, V. N., et al (2012). The properties and applications of nanodiamond. Nat Nanotechnol, Vol. 7, pp. 11-23.

83. Wang, H., Yang, Q., Niu C. H., Diamond Relat. Mater. 19 (2010) 441-444

84. Pentecost, A., Gour, S., Mochalin, V., Knoke, I., Gogotsi, Y., Deaggregation of Nanodiamond

Powders Using Salt- and Sugar-Assisted Milling. Applied Materials & Interfaces Vol. 2 (2010) pg. 3289-3294

85. Kruger, A.; Kataoka, F.; Ozawa, M.; Fujino, T.; Suzuki, Y.; Aleksenskii, A. E.; Vul, A. Y.; Osawa, E. Carbon 2005, 43, 1722-1730.

86. Kabana, K, Salvab, E., Akbugaa, J. Eur. Journal of Pharmaceutical Sciences xxx (2015) The effects of chitosan/miR-200c nanoplexes on different stages of cancers in breast cancer cell lines.

87. Bellich, B., D'Agostino, I., Semeraro, S., Gamini, A., Cesaro, A. "The Good, the Bad and the Ugly" of Chitosans. Mar. Drugs 2016, 14, 99

88. Ogawa, K, Effect of Heating an Aqueous Suspension of Chitosan on the Crystallinity of Polymorphs. Agric. Biol. Chem. 1991, 55, 2375-2379.

89. Ogawa, K.; Yui, T.; Okuyama, K. Three D Structures of chitosan. Int. J. Biol. Macromol. 2004, 34, 1-8.

90. Khan, M., Shahzad, N., Xiong, Li, T., Zhao, F., Siddique, N., Ali, M., Shahzad, H., Ullah, S., Rakha, A. Dispersion behavior and the influences of ball milling technique on functionalization of detonated nano-diamonds. Diam. Rel. Mater. 61 (2016), 32-40.

91. Xu, X. Y.; Zhu, Y. W.; Wang, B. C. Diamond Relat. Mater. 2005, 14, 206-212.

92. Zhu Y, Li J, Li W, Zhang Y, Yang X, Chen N, Sun Y, Zhao Y, Fan C, Huang Q. The Biocompatibility of Nanodiamonds and Their Application in Drug Delivery Systems. *Theranostics* 2012; 2(3):302-312. doi:10.7150/thno.3627. Available from http://www.thno.org/v02p0302.htm

93. Yu SJ, Kang MW, Chang HC. et al. Bright fluorescent nanodiamonds: no photobleaching and low cytotoxicity. J Am Chem Soc. 2005;127:17604-17605

94. Koppes, S., available at:

https://phys.org/news/2013-06-spintronics-approach-enables-quantum-technologies.html

95. Shenderova, O., Adamas Technologies, Inc., available at:

https://www.photonics.com/Article.aspx?AID=57396

96. Clark, GL; Smith, AF. X-ray diffraction studies. J. Phys. Chem. 1996, 40, 863-879.

97. Lee, A. V., Oesterreich, S., Davidson, N. E. MCF-7 Cells-Changing the Course of Breast Cancer Research and Care for 45 years J Natl Cancer Inst (2015) 107 (7)

98. Immaculate Heart of Mary Convent , Archive Notes . 2013 ; 4 (2)

99. Soule, H. D., Vazguez, J., Long, A., Albert S., Brennan, M., A human cell line from a plural effusion derived from a breast carcinoma . J Natl Cancer Inst . 1973 ; 51 (5): 1409 – 1416 .

100. Tuttle, T. M., Habermann E. B., Grund E. H., et al. Increasing use of contralateral prophylactic mastectomy for breast cancer patients: a trend toward more aggressive surgical treatment. J Clin Oncol. 2007;25:5203-9.

101. King T. A., Sakr R., Patil S., et al. Clinical management factors contribute to the decision for contralateral prophylactic mastectomy. J Clin Oncol. 2011;29:2158-2164.

102. Brennan M. E., Houssami N., Lord S., et al. Magnetic resonance imaging screening of the contralateral breast in women with newly diagnosed breast cancer: systematic review and meta-

analysis of incremental cancer detection and impact on surgical management. J Clin Oncol. 2009;27:5640-9.

103. Mignani, S., Bryszeska, M., Klajnert-Maculewicz, B., Zablocka, M., Majoral, J. Advances in Combination Therapies Based on Nanoparticles for Efficacious Cancer Treatment: An Analytical Report. Biomacromolecules 2015, 16, 1-27.

104. Hofree, M., Shen, J. P., Carter, H., Gross, A., Ideker, T. Nat. Methods 2013, 10, 1108-1115

105. Petros R. A., Desimone J. M. Strategies in the design of nanoparticles for therapeutic applications. Nature Reviews Drug Discovery 2010, 9:615-627.

106. Conner SD, Schmid SL: Regulated portals of entry into the cell. Nature 2003, 422:37-44.

107. Takei K, Haucke V: Clathrin-mediated endocytosis: Membrane factors pull the trigger. Trends in Cell Biology 2001, 11:385-391.

108. Bareford LM, Swaan PW: Endocytic mechanisms for targeted drug delivery. Advanced Drug Delivery Reviews 2007, 59:748-758.

109. Akinc A, Thomas M, Klibanov AM, Langer R: Exploring polyethylenimine-mediated DNAtransfection and the proton sponge hypothesis. Journal of Gene Medicine 2005, 7:657-663.

110. Dinçer S, Türk M, Pişkin E: Intelligent polymers as nonviral vectors. Gene Therapy 2005, 12:S139-S145.

111. Zhang ZY, Smith BD: High-generation polycationic dendrimers are unusually effective at disrupting anionic vesicles: Membrane bending model. Bioconjugate Chemistry 2000, 11:805-814.

112. Yamashiro DJ, Fluss SR, Maxfield FR: Acidification of endocytic vesicles by an ATP-dependent proton pump. Journal of Cell Biology 1983, 97:929-934.

113. Grabe M., Oster G.: Regulation of organelle acidity. Journal of General Physiology 2001,117:329-343.

114. Kamb, A; Wee, S.; Lengauer, C. Nat. Rev. Drug Discovery 2007. 6. 115-120

115. Holohan, C.; Van Schaeybroeck, S.; Longley, D. B.; Johnston, P.G. Nat. Rev. Cancer 2013, 13, 714−726.

116. Y. Zhu, Z. Yu, G.S. Shi, J.R. Yang, J.C. Zhang, W.X. Li, et al., Nanodiamonds act as Trojan horse for intracellular delivery of metal ions to trigger cytotoxicity, Part. Fibre Toxicol. 12 (2015) 2.

117. Qin et al.; Nanomaterials in Targeting Cancer Stem Cells for Cancer Therapy. Front. Pharmacol. (2017). 1-15

118. (5) (a) Wilczewska, Z. A.; Katarzyna, N.; Markiewicz, K. H.; Car, H. Pharm. Reports 2012, 64, 1020−1037. (b) Solaro, R.; Chiellini, F.; Battisti, A. Materials 2010, 3, 1928−1980. (c) Niemirowicz, K.; Car, H. CHEMIK 2012, 66, 868−881

119. Rojas S, Gispert JD, Martin R. et al. Biodistribution of amino-functionalized diamond nanoparticles. In vivo studies based on 18F radionuclide emission. ACS Nano. 2011;5:5552-5559

120. Jia NQ, Lian Q, Shen HB. et al. Intracellular delivery of quantum dots tagged antisense oligodeoxynucleotides by functionalized multiwalled carbon nanotubes. Nano Lett. 2007;7:2976-

2980

121. Chow, E. et al. Sci. Trans. Med. 3, 73ra21 (2011)

122. Zhu, Y., Li, W., Zhang, Y., Li, J., Liang, L., Zhang, X. et al. Excessive sodium ions delivered into cells by nanodiamonds: implications for tumor therapy, Small 8 (11) (2012) 1771–1779.

123. Chen, M., Pierstorff, E., Lam, R., Li, S., Huang, H., Osawa, E. et al., Nanodiamond mediated delivery of water-insoluble therapeutics, ACS Nano 3 (7) (2009) 2016–2022.

124. Mochalin, V. N., Shenderova, O., Ho, D., Gogotsi, Y. The properties and applications of nanodiamonds. Nature Nanotech. 7(2012) 11-23.